# Transient silencing of GLUT1, LDHA, and MCT4 affects glucose transport, glycolysis, and chemosensitivity in human pancreatic cancer cells

*by*

Kjersti Berg


Thesis for the degree: Master of Science
Molecular Biology and Biochemistry
60 credits

Department of Biosciences
Faculty of Mathematics and Natural Sciences

UNIVERSITY OF OSLO

April 2022

# Transient silencing of GLUT1, LDHA, and MCT4 affects glucose transport, glycolysis, and chemosensitivity in human pancreatic cancer cells

2022

Transient silencing of GLUT1, LDHA, and MCT4 affects glucose transport, glycolysis, and chemosensitivity in human pancreatic cancer cells

Kjersti Berg

http://www.duo.uio.no/

Print: Reprosentralen, Universitetet i Oslo

# Acknowledgements

The experiments performed in this thesis were undertaken at the Institute of Pharmacology at Rikshospitalet, funded by the Norwegian Cancer Society (Kreftforeningen), project number 212734-2019. The supervisors of this thesis were Manoj Amrutkar and Caroline Sophie Verbeke.

A special thank-you to Manoj Amrutkar for all guidance, help, and support during this whole period. I am extremely grateful for all the time you have spent helping and supporting me during both experimental lab work and thesis writing. A huge thank you to Caroline Sophie Verbeke for giving me the opportunity to work with this thesis and for supporting me through the whole process. Thank you, Anette Vefferstad Finstadsveen and Linda Trobe Dorg, for keeping me company in the lab and for guidance provided.

Finally, an enormous thank you to my family, particularly my dad Jonny, my boyfriend Anders, and my friends for believing in me and supporting me during this whole process.

April 2022

Kjersti Berg

# Abstract

Pancreatic ductal adenocarcinoma (PDAC), often referred to as pancreatic cancer is one of the most aggressive and deadliest cancer types, with a 5-year survival rate of less than 10%. PDAC is characterized by vague, non-specific symptoms, late detection, early metastasis, a high degree of heterogeneity, significant resistance to existing treatments, and a poor prognosis. A reprogrammed glucose metabolism is one of the hallmarks of pancreatic cancer. Pancreatic cancer cells (PCCs) take up large amounts of glucose and convert it into lactate independent of oxygen availability, a process called the Warburg effect, which leads to higher glucose needs. Thus, several metabolic proteins such as GLUT1, LDHA, and MCT4, responsible for glucose transport, lactate production, and lactate transport, respectively, are often overexpressed in PDAC. Evidence suggests the possibility of using GLUT1, LDHA, and MCT4 as prognostic markers and therapeutic targets for PDAC. However, the contribution of these glycometabolic proteins to the chemosensitivity of PDAC remains unknown. The aim of this study is to investigate the impact of GLUT1, LDHA, and MCT4 expression on glycolysis and chemosensitivity in human PCCs.

In this study, the expression of GLUT1, LDHA, or MCT4 was silenced for a short duration using siRNA-based transfections, and the impact of this on PCC glucose transport, glycolysis, viability, proliferation, and chemosensitivity was investigated using three different PCC lines (BxPC-3, Mia PaCa-2, Panc-1). Protein expression was determined by immunocytochemistry and western blot analysis. Phenotypic changes were determined by investigating MTT-based cell viability and proliferation by BrdU incorporation. Changes in glycolytic activity were determined using [$^3$H]-2-deoxy-D-glucose to measure glucose transport and the Glycolysis Cell-Based Assay Kit to measure lactate secretion. Lastly, chemosensitivity for gemcitabine and 5-fluorouracil (5-FU), reflected by drug-induced reduction in cell viability, was determined by MTT assay.

Expression analysis by immunocytochemistry and western blot analysis confirmed the successful silencing of GLUT1, LDHA, or MCT4, compared to the non-targeting control (NTC) in all three PCC lines. Discrete and mainly nonsignificant differences in viability and proliferation were observed when comparing the cells with suppressed GLUT1, LDHA, and MCT4 expression compared to NTC-transfected cells. Both BxPC-3 and Mia PaCa-2 showed

significantly higher reductions in glucose transport following GLUT1 silencing compared to NTC. GLUT1 silencing resulted in a significant decrease in lactate secretion in all three PCC lines. Compared to the other PCCs, Panc-1 showed higher lactate secretion upon silencing of LDHA or MCT4. When comparing the PCCs with silenced glycometabolic proteins to the NTC controls, treatment with Gemcitabine resulted in a small increase in cytotoxic effect in Mia PaCa-2 and Panc-1 with silenced LDHA or MCT4 when grown in normal glucose (NG) conditions, whereas all three cell lines remained resistant to Gemcitabine treatment when grown in low glucose (LG) conditions. Treatment with 5-FU had little to no impact on the viability of Mia PaCa-2 and Panc-1, both in LG and NG conditions, suggesting low 5-FU efficacy in these cell lines. In contrast, in BxPC-3, treatment with 5-FU resulted in a significant decrease in viability, both in LG and NG conditions. Furthermore, an increase in 5-FU sensitivity was observed in the cells with suppressed expression of LDHA or MCT4 as compared to NTC transfected cells both in LG and NG conditions.

In conclusion, a general trend of reduced glucose transport, lactate secretion, and unaffected or increased chemosensitivity was observed in PCCs with silenced GLUT1, LDHA, or MCT4 compared to PCCs transfected with NTC. However, it is important to note that the changes observed varied remarkably between the PCCs. Further investigation is needed to understand the underlying mechanisms that link chemoresistance with the changes induced by the silencing of GLUT1, LDHA, or MCT4.

# Table of Contents

# 1 Introduction

## 1.1 Pancreas

The pancreas is an approximately 14-23 cm long organ with an elongated shape, surrounded by the small intestine, stomach, liver, and spleen [1]. It is located behind the stomach and in the back (retroperitoneal) portion of the upper abdomen, with the tail in the left upper quadrant and the head in the right upper quadrant [2]. The anatomical structure of the pancreas is usually divided into five parts: head, uncinate process, neck, body, and tail. The head of the pancreas, the widest part of the pancreas, is outlined by the C-shaped loop of the duodenum that curves around it, and they are connected by connective tissues, while the tail is located near the hilum of the spleen [1, 2]. The body of the pancreas is centrally located and lies behind the stomach between the neck and tail of the pancreas. Beneath the body of the pancreas, the uncinate process, which is a hook-shaped projection of the head, is located [2]. A schematic illustration of the pancreas is shown in Figure 1.1.

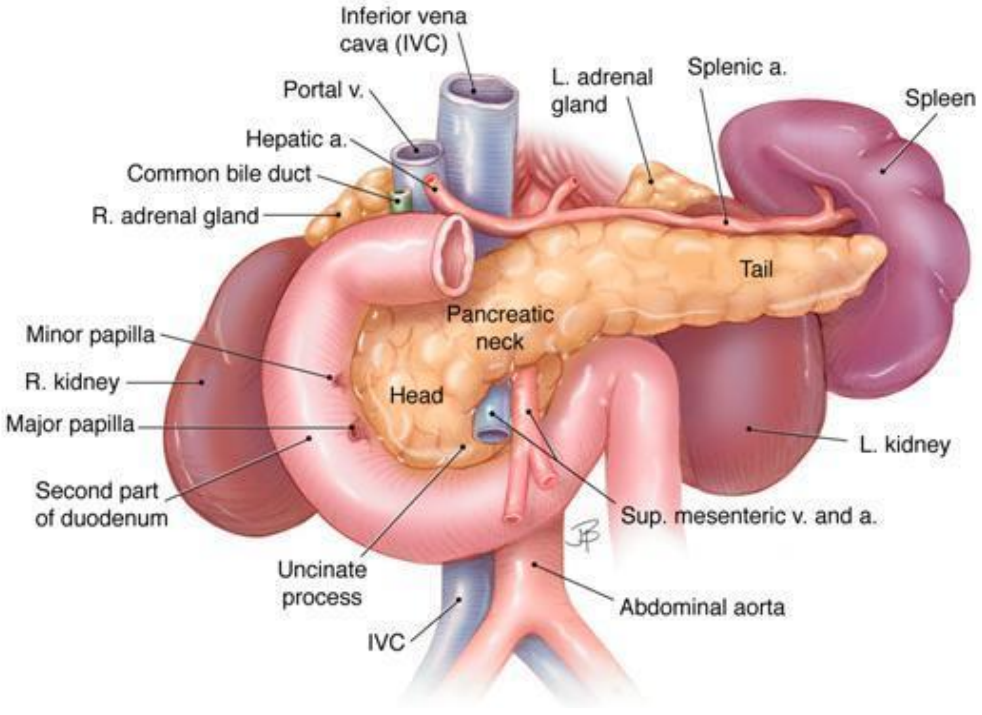


**Figure 1.1**: **Schematic figure of the anatomy of the pancreas and the relationship with the surrounding organs.** *The body of the pancreas is unlabeled in this figure due to its posterior location in the distal portion of the stomach between the neck and tail. This figure is taken from [2].*

The pancreas contains both exocrine (digestive) and endocrine (hormonal) glandular tissues. It is involved in both the gastrointestinal system and the endocrine system that, among other functions, maintains the homeostasis of glucose levels in the blood [1, 3]. The exocrine portion of the pancreas, which is responsible for the formation and secretion of digestive enzymes into the duodenum, comprises 98% of the pancreatic mass and has microscopic anatomy similar to the salivary glands with nest-like acini gathered in groups. Each acinus contains a single layer of epithelial cells surrounding a tiny lumen [3]. The head of the pancreas has a crucial anatomical relation with the duodenum, which is the first small part of the small intestine, and this is where the stomach empties the partially digested food into the small intestine, where the pancreas releases the digestive enzymes. The digestive enzymes include amylase (digestion of carbohydrates), trypsin and chymotrypsin (digestion of proteins), and lipase (break down of fats) [3, 4]. The secretions from the groups of acini, called pancreatic juice/fluid, travel through several branch ducts that come together in the central pancreatic duct. Another necessary duct, the common bile duct, originates in the liver and the gallbladder and secretes an essential digestive juice/fluid called bile. The common bile duct and the pancreatic duct are united in the duodenum, and both pancreatic juices/fluids and bile are released, and the body can digest carbohydrates, proteins, and fats [3-5].

The second important function of the pancreas is its endocrine function, which includes the formation and secretion of hormones necessary for regulating glucose levels in the blood. These hormones include insulin, glucagon, somatostatin, pancreatic polypeptide, and ghrelin, of which insulin and glucagon are the two main hormones of glucose regulation [1, 3, 4]. The endocrine part of the pancreas comprises only 1-2% of the total pancreatic mass and is made up of the islets of Langerhans. The islets vary in size, but the average diameter in humans is 100-150 μm. There are about 1 million islets in an adult human, where each islet contains approximately 2500 endocrine cells [3]. There are at least five different endocrine cell types identified, including α-cells, β-cells, δ-cells, PP-cells, and ε-cells [1, 4]. β-cells comprise 60-70% of the cells and produce insulin, while α-cells comprise approximately 20% of the endocrine cells and produce glucagon. Insulin is released by β-cells when the blood glucose levels are increased, while glucagon is released by α-cells when the blood glucose levels are decreased [3]. Thus, the pancreas can maintain the homeostasis necessary for normal glucose levels in the blood. Insulin inhibits glucagon secretion from α-cells, while the insulin secretion from β-cells is stimulated by glucagon, which is due to the close contact between the different cell types. δ-cells, which produce the hormone somatostatin that inhibits glucagon and insulin secretion, comprise approximately 10% of the cells, while PP-cells comprise <5% of the cells and produce the pancreatic polypeptide [1]. The physiologic function of the pancreatic polypeptide is unclear, but it has an inhibiting effect on the exocrine pancreas secretion [1, 3, 4].

## 1.2 Pancreatic Cancer

Cancer is defined as a neoplastic growth of cells that are derived from the body's normal tissues and can spread to distant organs to create new cancer cell colonies, so-called metastases. Primarily, cancer is caused by an accumulation of mutations and genetic alterations. These genetic alterations are either inherited from parent to offspring through germline or are somatically acquired through a cell's life cycle. Alterations in oncogenes, tumor suppressor genes, and DNA repair genes may lead to cancer development by allowing the cancer cells to escape the control mechanisms of growth and regulation [6]. Oncogenes are known as tumor-inducing genes that are overexpressed in cancer cells, while tumor suppressor genes are responsible for constraining cell proliferation and are often partially or entirely inactivated in cancer cells [6, 7].

The majority of malignant pancreatic neoplasms are pancreatic ductal adenocarcinomas (PDACs), cancers arising from the ductal cells of the exocrine portion of the pancreas. Pancreatic cancer is defined as a type of cancer that has its origin in the pancreas, and the majority arises from a microscopically small precursor lesion called pancreatic intraepithelial neoplasia (PanIN). Pancreatic cancer can also arise from larger precursor lesions such as intraductal papillary mucinous neoplasms (IPMNs) and mucinous cystic neoplasms [8]. Thus, PDAC is often referred to as pancreatic cancer, which also applies to this thesis [8-10].

## 1.3 Ductal Adenocarcinoma of the Pancreas

### 1.3.1 Epidemiology

Worldwide, pancreatic cancer is the fourth leading cause of cancer-related deaths for both genders, accounting for approximately 495 000 new cases and 466 000 deaths, according to GLOBOCAN 2020 estimates [11, 12]. Pancreatic cancer is ranked the third and fourth leading cause of cancer-related deaths in Northern America and Europe, respectively, according to the International Agency for Research on Cancer [13]. It is predicted that pancreatic cancer will become the second leading cause of cancer-related deaths in the western world during this decade [14]. Countries with a higher human development index, which is a measurement of human development based on health, knowledge, and standard of living, show a 4- to 5-fold higher incidence of pancreatic cancer, with the highest incidence rates in Europe, Northern America, and Australia/New Zealand [11]. According to the Norwegian Cancer Registry estimates, 929 new cases and 771 deaths due to pancreatic cancer were reported in 2020 in Norway [15].

### 1.3.2 Risk Factors

Both modifiable and non-modifiable risk factors affect the development of pancreatic cancer. The modifiable risk factors include smoking, the most important environmental risk factor, obesity, dietary factors, alcohol, and exposure to toxic substances. Chronic pancreatitis, an inflammatory condition in the pancreas that leads to fibrosis and loss of acinar and islet cells, as well as Helicobacter pylori or hepatitis C infections, are also associated with an increased risk of developing pancreatic cancer [16, 17]. On the other hand, non-modifiable risk factors include gender, age, ethnicity, diabetes mellitus, blood type, family history, and genetic factors [17, 18]. The incidence of pancreatic cancer worldwide is higher in men than in women, and 90% of the diagnosed patients are older than 55 years. The African-American population has a higher incidence of pancreatic cancer than Caucasians, likely due to differences in modifiable risk factors like alcohol consumption, smoking, and dietary factors [17, 18]. Several epidemiological studies have also shown that patients with blood type O have a significantly lower risk of developing pancreatic cancer than patients with blood type A, B, or AB [18]. Diabetes mellitus, both type 1 and type 2, is also a well-known risk factor for developing pancreatic cancer. Notably, pancreatic cancer can also be a risk factor for developing diabetes [16, 18]. Family history and genetic predisposition factors account for 5-10% of pancreatic cancers. If two or more first-degree relatives, that is, parents, siblings, or children, have been diagnosed with pancreatic cancer, it is familial pancreatic cancer [10, 17, 18].

### 1.3.3 Genetics

Alterations in several distinct pancreatic cancer genes are almost universal and occur in 70-98% of the cases [19]. The most frequent mutation in pancreatic cancer, which occurs in over 90% of the cases, is the missense mutations in the oncogene Kirsten rat sarcoma viral oncogene homolog (*KRAS*), particularly within codon 12 [16]. KRAS-mutation is found in approximately 95% of the earliest precursor lesions, the PanINs, which indicates that *KRAS* mutation is often the initiating genetic alteration for PDAC [20, 21].

Inactivation of tumor suppressor genes, particularly tumor protein 53 (*TP53*), mothers against decapentaplegic homolog 4 (*SMAD4* or *DCP4*), and cyclin-dependent kinase inhibitor 2A (*CDKN2A*), is part of the stepwise accumulation of genetic alterations needed for progression from PanINs to invasive and metastatic PDAC [20]. The tumor suppressor gene *TP53*, which encodes the transcription factor p53, induces senescence, which is a non-growing state resulting from cell cycle arrest, and apoptosis by transcriptionally activating target genes in the case of cellular stress such as DNA damage or oxidative stress. A loss-of-function mutation, which results in the loss of DNA binding ability and consequently gene transcription activation, is one of the most frequent mutations in all

types of cancer and occurs in 70% of pancreatic cancers [7, 19]. CDKN2A, which encodes the protein p16, regulates the cell cycle by inhibiting the complexes responsible for initiating the G1/S phase transition, cyclinD-CDK4, and cyclinD-CDK6. This gene is inactivated in approximately 30% of pancreatic cancers, and the resulting hyperactivation of CDK4/6 leads to the inactivation of the retinoblastoma (RB) tumor suppressor and thus promotes tumor progression [16, 19, 20, 22]. The tumor suppressor SMAD4, which is mutated in approximately 60% of pancreatic cancers, normally works as an intracellular mediator of the tumor growth factor-β (TGF-β) signaling pathway, which leads precursor cells into a less proliferative stage or induces apoptosis. Loss of SMAD4 can lead to a more aggressive phenotype, because the tumor suppressor activity is inactivated without affecting tumor response, and SMAD4 mutations are often associated with metastatic disease [20, 22].

Inherited genetic alterations account for 5-10% of pancreatic cancer cases. Examples of germ-line mutations and familial cancer syndromes associated with a higher risk for developing pancreatic cancer include, Peutz-Jeghers syndrome caused by a mutation in the tumor suppressor *STK11*, hereditary breast-ovarian cancer syndrome often caused by mutations in *BRCA1* and *BRCA2*, familial atypical multiple mole melanoma caused by a germline mutation in *CDKN2A*, Lynch syndrome caused by a mutation in the DNA-repair gene *MSH6*, hereditary pancreatitis caused by germ-line mutations in *PRSS1*. Mutations in other DNA-repair genes such as *MLH1*, *MSH2*, and *PALB2*, and mutations in for example ATM which is important for the DNA damage response, where germ-line mutations in *BRCA2* is the most frequent inherited risk identified in 5-17% of familial pancreatic cancer cases [16, 17].

### 1.3.4 Symptoms

A major problem with pancreatic cancer is the fact that there are few or no symptoms before the disease has progressed to an advanced stage, and 80-90% of patients are diagnosed with an unresectable tumor [17]. If symptoms are present, they are often non-specific, such as back pain, nausea, bloating, or change in stool, and this may delay the diagnosis because these symptoms usually are attributed to benign causes. The most frequent symptoms present at the time of diagnosis include abdominal pain (40-60%), abnormal liver function tests (~50%), jaundice (~30%), new-onset diabetes (13-20%), discomfort/pain in the upper abdomen, also called dyspepsia (~20%), nausea or vomiting (~16%), back pain (~12%), and weight loss (~10%) [16]. The location of the tumor within the pancreas also affects the disease presentation. Painless jaundice is a common symptom in tumors located in the pancreas head/neck due to biliary obstruction, while back pain is more likely in tumors located in the pancreas body due to anatomical location leading to the infiltration of local vascular structures like the celiac. However, tumors located in the pancreas tail often have no symptoms and

thus tend to be at an advanced stage at the time of diagnosis because the tail has fewer anatomical neighbors and tumors can grow more undisrupted [16, 17].

### 1.3.5 Diagnosis

The standard imaging technique used for diagnosis and staging of pancreatic cancer is triphasic pancreatic protocol computed tomography (CT). The CT can be used to detect the location of the tumor, whether blood vessels or organs surrounding the tumor have been infiltrated, and whether it has metastasized to the liver or lungs [23]. Other diagnostic tools available include abdominal ultrasonography, magnetic resonance imaging (MRI), and endoscopic ultrasound-guided fine-needle aspiration/biopsy for cytological/histological diagnosis [10, 17]. In addition, blood levels of cancer antigen 19-9 (CA19-9; also called carbohydrate antigen 19-9), a documented and validated serum biomarker for pancreatic cancer, can be measured in symptomatic patients, which may add weight to the diagnosis and may correlate with prognosis [16, 17, 23].

### 1.3.6 Treatment

The only potentially curative treatment for pancreatic cancer is surgical resection. However, only 15-20% of patients are diagnosed with resectable disease [10]. Even in the absence of metastasis, tumors are often classified as unresectable due to involvement of major blood vessel involvement, such as the celiac axis [24]. The 5-year survival rate is 20% in patients that present with a locally advanced, resectable tumor, which is still poor marks an increase from the overall 5-year survival rate of approximately 10% [16, 18, 23, 24].

The most common surgery, used for tumors located in the head of the pancreas, is a pancreatoduodenectomy (Whipple's procedure). The Whipple procedure includes the resection of both the pancreatic head and nearby organs which include the duodenum, proximal jejunum, common bile duct, gallbladder, and often the lower part of the stomach [16]. The Whipple's procedure is not performed if the tumor has grown extensively into blood vessels or has metastasized into other organs, most commonly liver or lungs. A distal pancreatectomy, which removes the body and/or tail region of the pancreas, is performed when the tumor is localized in the body or tail of the pancreas. In rare cases, the whole pancreas is removed with a total pancreatectomy [16, 23].

For the patients presenting with unresectable or metastatic disease, chemotherapy or radiotherapy are the only treatments available and are used to give life-prolonging and symptom-relieving effects. Chemotherapy is also used as neoadjuvant treatment before considering surgery if blood vessels are infiltrated [23]. The two most common valid first-line treatment options for advanced or metastatic

pancreatic cancer is gemcitabine combined with nanoparticle albumin-bound paclitaxel (Nab-paclitaxel, also known as Abraxane) and the combination FOLFIRINOX (made up of folinic acid, 5-fluorouracil, oxaliplatin, and irinotecan) [25]. Both treatment regimens are considered an option for patients with metastatic pancreatic cancer, depending mainly on the fitness of the patient. Which one of them is more effective in the individual patient is not exactly known due to the lack of predictive biomarkers [23, 25, 26].

## 1.4 The Microenvironment of Pancreatic Tumors

PDAC is characterized by a dense stroma, called desmoplastic stroma, which can comprise up to 80% of the total tumor volume [27, 28]. The stroma, which is very heterogeneous, comprises both cellular and acellular components. These components, which are collectively termed the tumor microenvironment (TME), include cancer-associated fibroblasts (CAFs), myofibroblasts, immune cells, pancreatic stellate cells (PSCs), extracellular matrix (ECM), pro-angiogenic factors, endothelial cells, non-essential amino acids, matrix metalloproteinases (MMPs), blood vessels, and soluble proteins like cytokines and growth factors, as illustrated in Figure 1.2 [28, 29]. The ECM is a vital non-cellular network which is present within all organs and tissues. Activated PSCs secrete large amounts of ECM components such as collagen (mainly type I, III, IV), laminin, fibronectin, and hyaluronic acid (HA), which is responsible for the physically firm and stiff PDAC tumor with an increased interstitial fluid pressure (IFP) that limits tumor permeability and vascular function. The increase in IFP leads to a hypoxic and nutrient-poor environment due to the limited vascular patency, and consequently, the reduced tumor perfusion and delivery of chemotherapeutic agents [30-33].

CAFs constitute one of the major cellular components of the TME and play an active role in cancer initiation, progression, and metastasis. The resident fibroblasts, particularly PSCs, are the main source of CAFs. The CAFs contribute to several important functions during tumor progression that includes production of ECM components, mediation of collagen cross-linking in the extracellular space to modulate tumor stiffness, secretion of multiple cytokines, chemokines, and growth factors, as well as inhibition of immune-effector cells and recruitment of immunosuppressive cells to allow cancer cells to evade immune surveillance [31, 34]. Two distinct subtypes of CAFs have been identified, namely myofibroblastic CAFs (myCAFs) and inflammatory CAFs (iCAFs). Moreover, recent studies have identified a third type of CAFs called antigen-presenting CAFs (apCAFs) [34].

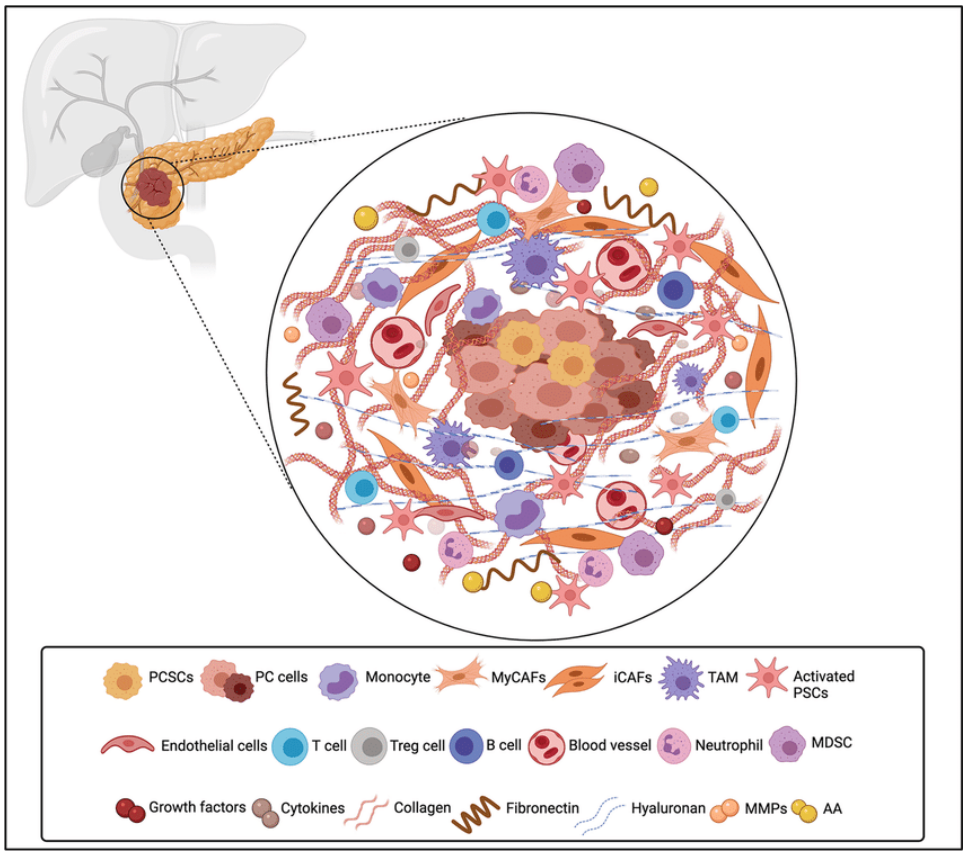


**Figure 1.2: Overview of the major components in the pancreatic tumor microenvironment (TME).** *The pancreatic TME mainly consists of pancreatic cancer cells, PSCs, CAFs, ECM components, immune cells, cytokines, pro-angiogenic factors, MMPs, non-essential amino acids, and growth factors. This figure is taken from [35]. PSC, pancreatic stellate cell; CAF, cancer associated fibroblast; ECM, extracellular matrix; MMPs, matrix metalloproteinases.*

myCAFs are characterized by an upregulated expression of a cluster of genes such as the myofibroblast genes *ACTA2*, which encodes α-smooth muscle actin (αSMA) and CTGF, as well as collagen type IV alpha 1 chains *COL1A1*, *COL5A1*, and *COL6A1*. myCAFs are primarily located adjacent to cancer cells in the peri-glandular region. The formation of myCAFs is induced by increased SMAD2 and SMAD3 phosphorylation, which indicates TGF-β signaling. myCAFs are thought to restrict tumor growth, but it is not clear how this is mediated [31, 34, 36]. On the other hand, iCAFs, which express high levels of interleukin-6 (IL-6) and several other inflammatory cytokines, leads to JAK/STAT activation through an IL-1 induced signaling cascade and promotes an inflammatory CAF state which is shown to promote tumor growth, neovascularization, and macrophage recruitment *in vivo*. During the formation of iCAFs, rapid phosphorylation of nuclear p65, which is a marker of nuclear factor-κB (NF-κB) activation, occurs and indicates a dependence on NK-κB. In contrast to myCAFs, iCAFs are located further away from the cancer cells in the desmoplastic areas of the tumor. Several chemokines that promote immunosuppression, including CXCL12, which

prevents T cells from entering the tumor, as well as CCL5, CCL2, and CCL17, which actively recruit CD4 regulatory T cells (Tregs) and monocytes, is secreted by iCAFs [27, 29-32, 37]. Lastly, apCAFs are shown to induce T-cell receptor (TCR) ligation in $CD4^+$ T cells and express MHC class II (MHCII)-related genes in an antigen-dependent manner. apCAFs are able to convert into myofibroblasts under convenient conditions, suggesting that CAFs represent a heterogeneous population with dynamic and interconvertible cell states [34].

### 1.4.1 Heterogeneity

PDAC has a high degree of heterogeneity that can occur either between different individuals with the same diagnosis (inter-tumor heterogeneity) or within the same tumor in the same patient (intra-tumor heterogeneity) [38]. In addition to cancer cell heterogeneity, several types of stroma exist. The abundance of stroma is an important variable parameter when observing inter-tumor heterogeneity. One activated stroma index, proposed by Erkan et al. [39], was dependent on the area occupied by collagen and the area occupied by αSMA+ stromal cells. High αSMA+ stromal cell infiltration and low collagen abundance were shown to have a worse prognosis, however, significant variations between tumors was observed [38, 39]. In addition, the functional heterogeneity and distribution of CAFs, including myCAFs, iCAFs, and apCAFs as described above, is also significant for the tumor outcome. Differences in the expression of stromal transcription factors such as SNAIL/ZEB1/ZEB2, as well as heterogeneity in inflammatory cell populations, also affect the tumor progression and outcome. Two different subtypes of stroma are identified, a “normal” type containing classical PSCs, and an “activated” type that comprises macrophages, metalloproteinase genes, and transcription factors. The “activated” subtype has shown to have a worse prognosis [38, 40]. In addition, intra-tumor heterogeneity can be either spatial, within the primary tumor, between different metastases, or within the same metastasis. Variable parameters within the microenvironment include the range of hypoxia, the pH gradient, and modulation of interactions and cell signaling between tumor and stromal cells [38, 40].

### 1.4.2 Pancreatic Stellate Cells (PSCs)

PSCs are the primary cellular component of the tumor microenvironment [35, 41]. Under normal conditions, PSC is quiescent and characterized by their ability to store retinoid, vitamin A and its analogues, usually in a form of lipid droplets that are scattered in the cytosol, which is crucial for the tissue homeostasis [42]. The presence of these vitamin A-containing droplets is a consistent marker for quiescent PSCs. The quiescent phenotype looks similar to the rough endoplasmic reticulum due to the collagen fibrils and lipid droplets containing vitamin A that surrounds the central nucleus, and the

phenotype is maintained by the level of vitamin A because it inhibits the expression of collagen, fibronectin, laminin, and αSMA [41-43]. Quiescent PSCs secrete MMPs such as MMP-2, -9, and -13 and their inhibitors, and are thus thought to be responsible for the turnover of ECM components. However, their physiological functions are still unclear [28, 42].

During cancerogenesis, the quiescent PSCs are transformed into active form, simply called the activated PSCs, which are characterized by increased proliferation, morphological changes, deposition of ECM, expression of αSMA, and loss of vitamin A-containing lipid droplets [29]. Activation factors of PSCs, which is secreted by platelets, endothelial cells, pancreatic acinar cells, or infiltrating cells like macrophages, includes the response to inflammatory mediators, alcohol metabolites, and growth factors like the platelet-derived growth factor (PDGF), as well as TGF-α and TGF-β [42]. The activated PSC phenotype resembles fibroblasts with a spindle-like shape and shows an increased ability to proliferate and migrate. Associated with the loss of the vitamin A-containing droplets, activated PSCs show an increased production of collagen type I and III, fibronectin, hyaluronic acid, and laminin [41-43]. Interactions between PSCs and pancreatic cancer cells maintain the desmoplastic reaction, which means a pervasive growth of dense fibrous tissue. This results in a hypoxic, nutrient-poor microenvironment as described above. Thus, PSCs provide the perfect environment for pancreatic tumor cells, facilitate their metastasis, and provide protection against chemotherapy and other anti-tumor therapies. In addition, recent studies have shown that PSCs may be important for PDAC metabolism due to the secretion of non-essential amino acids, particularly alanine. Due to the dense stroma, PDAC cells have limited access to glucose and glutamine-derived carbon, and alanine can be used as an alternative carbon source in the TCA cycle [42].

# 1.5 Cell Metabolism

## 1.5.1 Metabolism

Metabolism includes the sum of all chemical reactions that are vitally essential and occur within the cells all throughout the body. The chemical reactions can be divided into anabolism and catabolism, which means the synthesis and degradation of complex macromolecules like nucleic acids, lipids, polysaccharides, and proteins to simpler molecules like carbon dioxide ($CO_2$), ammonia, and water, respectively. Living organisms require energy continuously to maintain both cellular and whole-body function, and metabolic pathways are essential for either maximizing the capture of energy or minimizing the use of energy [44].

## 1.5.2 Glucose Metabolism

Glycolysis, also known as the Embden-Meyerhof pathway, is a metabolic pathway that ultimately results in the splitting of glucose into two pyruvate molecules in the cytosol of cells. The pathway does not require oxygen but is the first step of cellular respiration. Glycolysis can be divided into two phases, the "investment" phase, where the input is 2 adenosine triphosphate (ATP) molecules and 1 glucose molecule, and the "payoff" phase, where the net output is 2 ATP, 2 nicotinamide adenine dinucleotide (NADH), and 2 pyruvate molecules. All the 10 steps in glycolysis are catalyzed by their own enzyme with phosphofructokinase as the most essential regulating enzyme due to its rate-limiting abilities [45].

The first step of the "payoff" phase includes the metabolizing of G3P into 1,3-diphosphoglycerate by using the enzyme glyceraldehyde-3-phosphate dehydrogenase (GAPDH) which reduces NAD+ into NADH and $H^+$. In the next step, the first two ATP molecules are created by the loss of one phosphate group when phosphoglycerate kinase (PGK1) is used to transform 1,3-diphosphoglycerate into 3-phosphoglycerate. Two ATP molecules are produced at this step because there were two 3-carbon sugars at the beginning of the "payoff" phase, and each 3-carbon molecule produces one ATP molecule. Phosphoglycerate mutase (PGM) is used to transform 3-phosphoglycerate into 2-phosphoglycerate before enolase converts 2-phosphoglycerate to phosphoenolpyruvate (PEP) and release one $H_2O$ molecule. In the last step, which is irreversible, PEP is converted into pyruvate by the enzyme pyruvate kinase. The last step also phosphorylates adenosine diphosphate (ADP) into ATP and creates the last two ATP molecules, one for each 3-carbon molecule. 4 ATP molecules are created in total during glycolysis, but the net output is 2 ATP molecules because the "investment" phase uses two [45].

To keep the glycolysis running, NADH needs to be recycled back to NAD+. This is achieved by oxidative phosphorylation in the mitochondria of aerobic cells and by fermentation, either lactic acid or alcohol fermentation, in anaerobic cells. Pyruvate, produced in glycolysis, is oxidized to form acetyl coenzyme A (CoA) that can enter the tricarboxylic acid cycle (TCA cycle) under aerobic conditions. The TCA cycle produces three NADH molecules and one dihydroflavine-adenine dinucleotide ($FADH_2$) molecule, which is transferred to complex I and complex II, respectively, of the electron transport chain (ETC) where they are used as electron donors, as well as two $CO_2$ molecules. The electrons transferred by the ETC are ultimately used to convert ADP to ATP molecules by oxidative phosphorylation (OXPHOS). Aerobic respiration, which includes glycolysis, the TCA cycle, the ETC, and OXPHOS, efficiently maximizes the conversion of ATP, which is an important chemical energy carrier used in many biological processes, from nutrient energy due to the strong oxidative abilities of $O_2$. The total number of ATP produced by aerobic respiration varies from 30-38 ATP molecules

among different sources [44-49]. An overview of the anabolic pathways of glucose metabolism is illustrated in Figure 1.3.

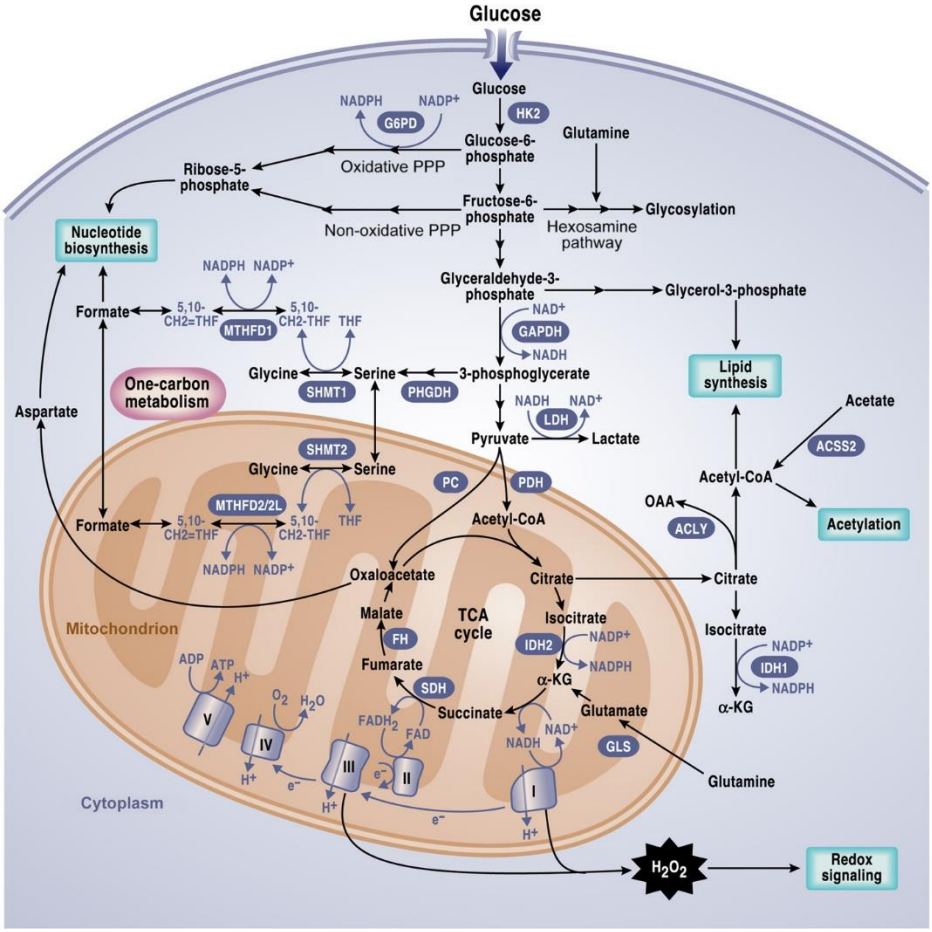


**Figure 1.3: An overview of the anabolic pathways of glucose metabolism.** *Glucose is transported into the cytoplasm and is converted to pyruvate by glycolysis before pyruvate is either fermented into lactate or transported into the mitochondria where it is fed into the TCA cycle. NADH and $FADH_2$, produced during the TCA cycle are transferred to the ETC and used to convert ADP to ATP during OXPHOS. This figure is taken from [50]. TCA cycle, tricarboxylic acid cycle; NADH, nicotinamide adenine dinucleotide; $FADH_2$, flavin adenine dinucleotide; ETC, electron transport chain; ADP, adenosine diphosphate; ATP, adenosine triphosphate; OXPHOS, oxidative phosphorylation.*

Under anaerobic, or hypoxic, conditions however, the pyruvate produced by glycolysis is not transferred into the mitochondria to participate in the TCA cycle. Instead, pyruvate is converted into lactate by the enzyme lactate dehydrogenase (LDH) in the cytosol. Lactate fermentation is able to regenerate the required NAD+ from NADH but is not a direct energy source for the cells. Thus, the only ATP produced in this reaction is the two ATP molecules produced from glycolysis [51].

## 1.6 Cancer Metabolism

Reprogrammed metabolism, described as alterations in the metabolic activities of cancer cells that support their malignant properties and differ from normal cells, is observed in many cancer cell types and is considered a hallmark of cancer [50]. Altered metabolism in cancer cells affects all stages of cell-metabolite interaction, and often either allows cells to proliferate and grow at elevated levels or supports the cell survival under stressful conditions. The reprogramming of metabolism has been organized into the following six hallmarks: metabolic interactions with the microenvironment, alterations in metabolite-driven gene regulation, increased demand for nitrogen, use of glycolysis/TCA cycle intermediates for biosynthesis and NADPH production, use of opportunistic modes of nutrient acquisition, and deregulated uptake for glucose and amino acids. Different types of cancer cells usually do not display all hallmarks, but most contain several alterations [50, 52].

### 1.6.1 The Warburg Effect/Aerobic Glycolysis

The Warburg effect, also called aerobic glycolysis, is a classic example of reprogrammed metabolism. In normal tissues, glycolysis is the physiological response to hypoxia. In cancer cells however, Otto Warburg observed that lactate fermentation occurred regardless of oxygen availability [50]. Energetically, the utilization of aerobic glycolysis makes little sense for cancer cells because glycolysis only yields two ATP molecules, while aerobic respiration via OXPHOS yields 30-38 ATP molecules. The inefficient glucose metabolism of cancer cells results in the requirement of importing enormous amounts of glucose into the cells. Thus, cancer cells express elevated levels of different glucose transporters, especially glucose transporter 1 (GLUT1). GLUT1 drives the high glucose uptake in cancer cells by spanning over the plasma membrane. In addition, glycolytic intermediates are able to supply subsidiary pathways to support the metabolic demands of proliferating cells due to the increased glycolytic flux [7, 50, 53].

## 1.7 Glucose Metabolism in Pancreatic Cancer

Reprogrammed metabolism plays a critical role in pancreatic cancer tumorigenesis, with altered glycolysis as the major metabolic alteration. In addition to glycolysis, there are several important metabolic pathways that branch out from glycolysis that are also known to promote tumorigenesis, including pentose phosphate (PPP), hexosamine biosynthesis (HBP), serine biosynthesis, and TCA cycle [54]. The dominant driver for metabolic reprogramming in PDAC is the oncogene *KRAS*, which is mutated in over 90% of cases, as well as other canonical oncogenes like *AKT*, *MYC*, and *PI3K*, and tumor suppressors like *TP53*, *RB*, and *PTEN* [53-55]. Upregulated expression of glucose transporters,

particularly GLUT1, and rate-limiting glycolytic enzymes such as HK2, PFK1, and lactate dehydrogenase A (LDHA) is often associated with a worse prognosis of PDAC [49]. For PDAC progression, overexpression of monocarboxylate transporter 1 (MCT1) and particularly MCT4, which is essential for the prevention of intracellular lactate accumulation, is critical for the mobilization and excretion of potentially toxic byproducts [55]. Of all different glycometabolic regulators, this study focuses on understanding the role of GLUT1, LDHA, and MCT4, which are critical in pancreatic cancer context.

In addition to altered glycolysis, enhanced glucose metabolism can promote PDAC tumorigenesis by several mechanisms mediated by pathways branched out from glycolysis. These include new biomass support (PPP and serine biosynthesis), providing ATP and other forms of energy (glycolytic flux and TCA cycle), reactive oxygen species (ROS) maintenance (glutamine metabolism and TCA cycle), signal modulation (HBP), nucleotide biosynthesis (PPP), lipid glycosylation (HBP), and DNA methylation (serine biosynthesis) [53-55]. *Autophagy*, which is the process of recycling cellular components from damaged cells, and *macropinocytosis*, which is a nonspecific uptake of extracellular components, are two salvage pathways important for scavenging critical metabolites important for fast proliferation and division of cancer cells [54].

### 1.7.1 Glucose Transporter 1 (GLUT1)

One of the rate-limiting steps of glucose metabolism is the transport of glucose across the plasma membrane. Facilitated transporters (GLUTs), particularly GLUT1 in PDAC, play an important role in mediating the transport and increased expression of these transporters leads to enhanced glucose uptake. GLUT1, encoded by the gene *SLC2A1*, transports glucose across a hydrophobic cell membrane in an ATP-independent manner down its concentration gradient [54]. In normal and benign tissues, GLUT1 expression is commonly undetectable, while a significant overexpression is observed during tumorigenesis. Activation of the oncogene *KRAS* is likely associated with the overexpression of GLUT1 in PDAC as *KRAS* silencing in a genetically engineered mouse model with the expression of mutant *KRAS* under a deoxycycline-inducible promoter showed decreased glucose uptake *in vivo*, as well as downregulation of GLUT1 and several glycolytic enzymes [55]. Paraoxonase 2 (PON2), which is a lactone hydrolyzing enzyme, regulates GLUT1-mediated glucose transport and promotes PDAC growth by directly interacting with GLUT1 via the membrane protein stomatin [54, 56, 57]. GLUT1 has been investigated as a potential prognostic biomarker of PDAC, but conflicting results were observed among different studies. These are some inconsistent reports showing a correlation between overexpressed GLUT1 and poor survival. However, due to the critical role of GLUT1 in PDAC progression, investigating the prognostic value further could be meaningful [54, 58].

### 1.7.2 Lactate Dehydrogenase A (LDHA)

LDHA is a rate-limiting glycolytic enzyme responsible for converting pyruvate to lactate, which is especially important because PDAC tumorigenesis is dependent on aerobic glycolysis, or the Warburg effect, as described above. Overexpressed LDHA, which promotes cell proliferation, migration, and invasion, is often observed in PDAC, and is commonly associated with tumor size, tumor stage, and prognosis [54, 59]. Hypoxia-inducible factor (HIF) is the major transcription factor mediating cell response to hypoxia, and the expression level of HIF-1 directly correlates with the expression of LDHA. However, the underlying molecular mechanisms mediating the interaction between LDHA, and HIF-1 remains unclear [59]. In addition, transcription factors like KLF4 and FOXM1 are also shown to promote the transcriptional upregulation of LDHA in PDAC to induce glycolysis [54]. Similar to GLUT1, LDHA is also being investigated as a potential prognostic biomarker and therapeutic target for PDAC [59].

### 1.7.3 Monocarboxylate Transporter 4 (MCT4)

MCT4, encoded by the gene *SLC16A3*, is one of two major lactate transporters, the other being MCT1, that are extensively expressed in PDAC cells. MCT4 is known to be activated by *KRAS* signaling. Enhanced lactate transportation is critical for maintaining cytosolic pH levels and preventing the toxic effects of intracellular lactate accumulation in PDAC cells [54, 55]. In addition, the export of lactate promotes the reduction of pyruvate to lactate, as well as the oxidation of nicotinamide adenine dinucleotide (NADH) to $NAD^+$ which is an important coenzyme for the maintenance of continued glycolysis and oxidation of glyceraldehyde 3-phosphate [54]. Cluster of differentiation 147 (CD147) is the glycoprotein responsible for the membrane localization of both MCT1 and MCT4, and decreased levels of CD147 result in lactate accumulation and reduced PDAC growth [54, 60]. Due to the ability of promoting tumor growth and survival under stressful conditions, MCT4 could be a potential therapeutic target and prognostic marker for PDAC [60, 61].

## 1.8 Gene Silencing

### 1.8.1 Central Dogma of Molecular Biology

The flow of genetic information within a biological system is explained by the central dogma of molecular biology. “Information” in this context refers to the precise determination of sequence, either of bases in the nucleic acid or amino acid residues in the protein. The central dogma states that this

information cannot be transferred back from protein to either protein or nucleic acid, as stated by Francis Crick in 1957 and then re-stated by Crick in a Nature paper published in 1970. DNA, RNA, and protein are the three major classes of information-carrying linear biopolymers in which sequence information is transferred between living organisms. Among the nine conceivable direct transfers possible, three transfers normally occur in most cells, called the three general transfers. Three special and three unknown transfers also exist, but these are much less common and will not be discussed here. The three general transfers are as follows: i) DNA replication - the process where two identical copies or replicas of DNA are synthesized by using an existing DNA molecule as their template; ii) transcription - the process where a complementary RNA molecule is synthesized by using a DNA strand as the template; and iii) translation - the ribosome-mediated process that includes the assembly of a polypeptide with the amino acid sequence specified by the nucleotide sequence of an mRNA molecule [46, 62].

### 1.8.2 Altering the Gene Expression

The expression of a particular gene can be altered experimentally in two directions: overexpression and silencing/knockdown. The overexpression experiment is used as a qualitative experiment to identify novel proteins involved in the biological processes of interest, and study their function [63]. By using overexpression experiments, a particular protein, complex, or pathway can either be activated or inhibited in two major categories of methods - inhibition and activation can result in an overexpressed phenotype. Overexpression of a protein that inhibits the protein of interest (PoI) is a straightforward way to reduce the amount of PoI. For example, degradation of the hTERT telomerase subunit can be achieved by overexpressing the mammalian ubiquitin E3 ligase MKRN1 [64]. The second major type of overexpression mechanism is activating a step in a pathway that activates PoI. This can be achieved by either overexpressing a key regulatory step that leads to the activation of the pathway of interest or overexpressing an utterly inactive gene and causing an overexpressed mutant phenotype [63, 64].

The thesis focuses on the silencing aspect of gene alteration, in which previously active genes can be inactivated by an epigenetic modification of gene expression referred to as gene silencing. Under normal development and differentiation, gene silencing is used to suppress genes or chromosomal regions in cell types or tissues where they are not needed. Gene silencing is mediated by several mechanisms, including changes in DNA methylation levels, chromatin compaction, alterations in covalent modifications of histone proteins, or destabilization of mRNA [65]. Gene silencing forms large domains of DNA that are unapproachable to DNA binding proteins in a regional manner rather than being promoter- or sequence-specific. In addition, the silent chromatin regions are inheritable because they stay persistent during mitotic and meiotic cell divisions to ensure their chromatin

structure is replicated during chromosome duplication, a process commonly known as an epigenetic inheritance [66]. Small RNA regulators, like microRNAs (miRNAs) and small interfering RNAs (siRNAs), mediate the mRNA destabilization and suppression of mRNA translation and are commonly used in gene silencing methods [65]. Other gene silencing methods include SIR-mediated gene silencing in budding yeast, which is a multiprotein nucleosome binding complex, and HP1- and Swi6-based silencing mechanisms, which are structural components of heterochromatin and silent chromatin domains, respectively [66].

There are three major gene delivery systems used in both overexpression and silencing experiments called - transformation, transduction, and transfection. *Transformation* is described as a series of events resulting in a permanent change in phenotype and is commonly used to investigate non-viral DNA transfer in non-animal eukaryotic cells, plant cells, and bacteria. *Transduction* refers to the process of infecting a cell with an isolated viral nucleic acid from either a bacteriophage or a eukaryotic virus and is commonly used to investigate virus-mediated DNA transfer [67]. *Transfection*, the key technique used in this thesis, refers to the introduction of nucleic acids (DNA or RNA) into cells to change the cellular properties and make it possible to study protein expression and gene function within the cells. Two major types of transfection are commonly used: stable transfection and transient transfection [67, 68].

### 1.8.3 Transient *versus* Stable Transfection

Stable transfection refers to the process of integrating a DNA plasmid into cells for long-term. Because the DNA is commonly integrated into the cellular genome, the introduced DNA is passed on to future generations of the cells. To successfully perform stable transfection, a selectable marker to select the cells that have acquired the DNA, as well as effective DNA delivery, is required. It is sometimes hard to predict which regions that are integrated into the cells contain the gene of interest. One commonly used way to solve this problem is to develop a gene with antibiotic resistance within the DNA plasmid. This way, only the stably transfected cells will expand, and the non-stable cells will die with continued antibiotic treatment. However, this type of transfection is a complex procedure, time-consuming, and costly effort, and thus, its use is limited [67-69].

In contrast, transient transfection, in which DNA is introduced into the cells for short-term and can be detected for the duration of up to 7 days. However, the cells are typically harvested 24-96 hours from transfection initiation for experimental purposes. Unlike stable transfection, the transfected DNA is not integrated into the cellular genome during transient transfection and is thus not passed on to the future generations and is observed within the cells for a shorter duration. The use of supercoiled plasmid DNA leads to the most efficient transient transfection, but siRNAs, miRNAs, mRNAs, and

even proteins can also be used. Transfected DNA is transported into the nucleus, while transfected RNA remains in the cytosol. By using transfected RNA, it is either expressed almost immediately after transfection by using mRNA or bound to mRNA and used to silence the expression of a particular gene by using siRNA or mRNA [68, 70]. In this thesis, the silencing of three key glycometabolism-related genes (GLUT1, LDHA, and MCT4) was performed using siRNA-based transient transfection.

## 1.8.4 Transient Gene Silencing using siRNA

To induce short-term silencing of target genes, the most commonly used RNA interference (RNAi) tool is siRNA [71]. In RNAi, double-stranded RNA (dsRNA) causes the degradation of complementary mRNA when introduced into the cell. siRNA is formed in the cells by a ribonuclease known as Dicer, which cleaves the long dsRNAs. An RNA-induced silencing complex (RISC) is then formed by the reassembling of siRNAs and protein complements, and the activated RISC is by base-pairing interactions between the mRNA and the siRNA antisense strand bound to a complementary transcript. This leads to the cleavage of the bound mRNA, and the degradation results in gene silencing, which means the inactivation of targeted genes. This is advantageous to investigate the impact of these particular genes of interest [72, 73]. A schematic figure of the mechanism is shown in Figure 1.4.

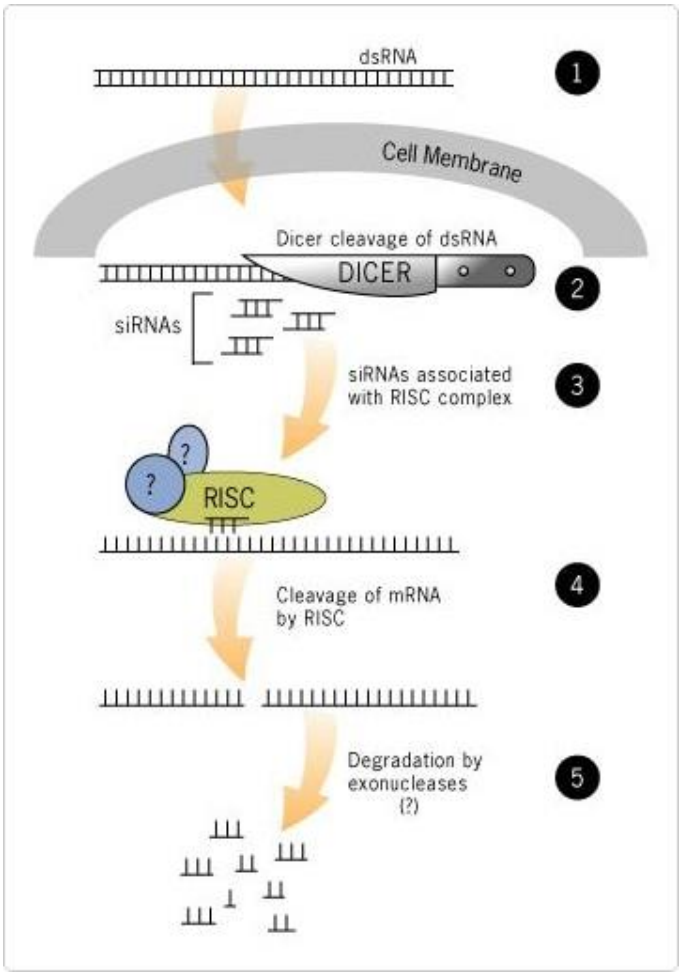


**Figure 1.4: Schematic overview of the RNAi mechanism used for gene specific silencing.** *This figure is taken from [72]. RNAi, RNA interference; dsRNA, double stranded RNA; mRNA, messenger RNA; RISC, RNA-induced silencing complex.*

# 1.9 Chemosensitivity

Pancreatic tumors are known for their strong resistance to chemotherapy, referred to as chemoresistance. Such resistance limits the efficacy of chemotherapy and can either be ineffective from the start of treatment due to genetic factors, known as intrinsic (de novo or innate) resistance, or become ineffective after being exposed to the treatment for a certain period of time due to genetic or epigenetic alterations, known as acquired resistance [74]. In addition, the dense stroma present in pancreatic tumors is thought to be associated with intrinsic chemoresistance, because it presents a barrier to drug delivery [75].

## 1.9.1 Gemcitabine

Gemcitabine (2',2'-difluoro 2'-deoxycytidine, dFdC) has been the cornerstone for PDAC treatment of all stages for more than two decades since its first use in 1996. Gemcitabine is a nucleoside analog of deoxycytidine that displays distinctive anti-proliferative properties that depend on inhibitory actions on DNA synthesis. Compared to other cytotoxic agents, gemcitabine is more efficient on pancreatic cancer cells. However, the PDAC prognosis remains poor due to the fact that chemoresistance is often developed within a few weeks of treatment initiation [74, 76-78].

Gemcitabine is a prodrug, which means it is a molecule with little to no pharmacological activity that needs to be converted into its active drug metabolites through cellular uptake and intracellular phosphorylation. Due to the hydrophilic nature of the molecule, gemcitabine transport into the cells is processed by different human nucleoside transporters (NTs). These NTs include the cation-dependent human concentrative nucleoside transporters (hCNTs) and the energy-independent human equilibrative nucleoside transporters (hENTs) that contain the solute carrier families SLC28 and SLC29, respectively. Gemcitabine is primarily transported into the pancreatic cancer cells by hENT1 and, to some extent, by hENT2, hCNT1, and hCNT2 [74, 76, 77, 79].

Once inside the cell, gemcitabine is phosphorylated into gemcitabine monophosphate (dFdCMP) by deoxycytidine kinase (dCK), which is further phosphorylated into the active drug metabolites gemcitabine diphosphate (dFdCDP) and gemcitabine triphosphate (dFdCTP) by pyrimidine nucleoside monophosphate kinase (NMPK) and nucleoside diphosphate kinase (NDPK), respectively. dFdCTP, being the competitive substrate of deoxycytidine triphosphate (dCTP) and an inhibitor of DNA polymerase, is incorporated into DNA during replication and added to the elongated DNA strand and thus inhibits the chain elongation of DNA because DNA polymerase is unable to proceed, and exonucleases are unable to remove gemcitabine from this position. This process, called masked chain termination, results in gemcitabine-induced apoptosis, or programmed cell death [74, 76, 77, 80].

Chemoresistance to gemcitabine is increased by several metabolism pathways, including activating and inactivating enzymes, drug transporters, and competitive substrates to active metabolites [74]. Decreased levels of the drug transporters hENT1, hCNT1, and hCNT3, and the enzyme dCK responsible for phosphorylating the prodrug inside the cells, are associated with an increased chemoresistance to gemcitabine and an overall poorer prognosis. In contrast, cytidine deaminase (CDA) – a gemcitabine inactivating enzyme, which is responsible for the deamination of dFdC to the uracil metabolite dFdU, which is not a substrate for pyrimidine nucleoside phosphorylases and are degraded and excreted out of the cells. The M1 subunit of ribonucleotide reductase (RRM1), which provides a binding site for DNA synthesis enzyme regulation correlates with increased chemoresistance to gemcitabine when upregulated [74, 77, 80].

### 1.9.2 5-Fluorouracil (5-FU)

5-fluorouracil (5-FU) is another important anti-cancer drug against pancreatic cancer. It is often combined with leucovorin, oxaliplatin, and irinotecan in a therapeutic regimen referred to as FOLFIRINOX [16, 78]. Compared with gemcitabine monotherapy, 5-FU is shown to be valuable in combination therapy. However, chemoresistance, which is induced by several factors, including alterations of the target, activation of DNA repair pathways, poor drug uptake, resistance to apoptosis and the TME, and high cytotoxicity, still remains a serious concern [81].

The efficiency of 5-FU is dependent on the transport system because it targets intracellular enzymes. Because 5-FU is an analog of the pyrimidine uracil, it is transported into the cells with the same transport system used by the uracil. Similar to gemcitabine, 5-FU is also a prodrug and is converted to several active metabolites once inside the cells, including fluorodeoxyuridine monophosphate (FdUMP), fluorodeoxyuridine triphosphate (FdUTP), and fluorouridine triphosphate (FUTP). The anti-cancer effects of 5-FU provided by these active metabolites include the inhibition of the intracellular enzyme thymidylate synthase (TS) and the incorporation of its metabolites into RNA and DNA [81-83]. The role of TS is to catalyze the reductive methylation of deoxyuridine monophosphate (dUMP) to deoxythymidine monophosphate (uTMP) with the 5,10-methylenetetrahydrofolate ($CH_2THF$) as the methyl donor. This leads to an imbalance in the deoxynucleotide pool, which significantly disrupts the DNA synthesis and repair, leading to lethal DNA damage to the cancer cells [81, 82]. In addition, the active 5-FU metabolite FUTP is broadly incorporated into RNA, where it disrupts normal RNA processing and function [82, 83].

Resistance against 5-FU is mainly focused on the key enzyme TS, and overexpression of this enzyme prior to treatment commonly leads to intrinsic resistance because 5-FU efficiency is dependent on TS inhibition. The availability of the methyl donor $CH_2THF$ also affects the chemosensitivity of 5-FU.

The absence of $CH_2THF$ leads to poor inhibition of TS because the active metabolite FdUMP forms an unstable binary complex. Acquired resistance can occur due to gene amplification and mutations in the TS gene. In addition, the effects of TS deficiency can be relieved due to the restoration of thymidylate from thymidine by the enzyme thymidine kinase [84, 85]. Another factor that could affect the chemosensitivity of 5-FU is the rate-limiting enzyme of 5-FU catabolism dihydropyrimidine dehydrogenase (DPD), which converts 5-FU to dihydro-fluorouracil (DHFU). Due to the abundant expression of DPD in the liver, most (over 80%) of the administered 5-FU is catabolized there. Patients with low DPD levels or a DPD deficiency could be more sensitive to 5-FU treatment but are at higher risk of developing severe 5-FU toxicity [81, 82, 84, 85].

# 2 Aim of the Study

Reprogrammed glucose metabolism and chemoresistance are two hallmarks of pancreatic cancer. Both processes are considered adaptive, and they are altered during tumor development. Glycometabolic changes in pancreatic cancer can vary depending on the energy needs of the tumor, and they can also be affected during chemotherapy treatment. Over the years, extensive research has been carried out to investigate the alterations in glycometabolim and chemoresistance and the underlying mechanisms in PDAC. However, it remains unknown whether both processes are entirely independent or whether they are interlinked and have any mutual advantages to the survival of the cancer cells. The aim of the thesis is to investigate the potential links between glycometabolism and chemosensitivity in pancreatic cancer. For this purpose, three key regulators of pancreatic glycometabolism, namely, GLUT1, LDHA, and MCT4, were studied in human pancreatic cancer cell lines (BxPC-3, Mia PaCa-2, and Panc-1). Using an siRNA-based gene silencing approach, the impact of glycometabolic regulators on glucose transport, glycolysis, cell growth, and chemosensitivity was investigated.

Hypothesis: Reduced expression of GLUT1, LDHA, and MCT4 may affect growth, glucose metabolism, and chemosensitivity in pancreatic cancer cells.

# 3 Methods and Materials

## 3.1 Cell Lines

In this study, three commercially available and commonly used pancreatic cancer cell (PCC) lines BxPC-3 (#CRL-1687™), Mia PaCa-2 (#CRL-1420™), and Panc-1 (#CRL-1469™), were used. All three cell lines are adherent cells. These cell lines were derived from primary pancreatic tumors and were resourced from the American Type Culture Collection (American Type Culture Collection, ATCC, Manassas, VA, USA). Original cell lines were cultured and expanded by colleagues in the laboratory, and their aliquots were stored in liquid nitrogen ($N_2$) vapors container until further use. Relevant information about the cell line origin and (including the source information) the cell line characteristics is presented in Table 1, and further detailed information is available at ATCC's website (https://www.atcc.org) [86, 87].

**Table 1:** Cell line characteristics and donor information [86].

| Cell Line | Age/Gender | Doubling Time | Differentiation | Metastasis | Mutations |
|---|---|---|---|---|---|
| BxPC-3 | 61 (F) | 48-60 hrs | Moderate to poor | No | KRAS: WT<br>P53: 220 Cys<br>CDKN2A: WT<br>SMAD4: HD |
| Mia PaCa-2 | 65 (M) | 40 hrs | Poor | ND | KRAS: 12 Cys<br>P53: 248 Trp<br>CDKN2A: HD<br>SMAD4: WT |
| Panc-1 | 56 (F) | 53 hrs | Poor | Yes | KRAS: 12 Asp<br>P53: 272 His<br>CDKN2A: HD<br>SMAD4: WT |

F = Female; M = Male; ND = Not determined; WT = Wild type; HD = Homozygous deletion

## 3.2 Cell Culture Medium

All three PCC lines indicated above were cultured and maintained in a complete growth medium. Major components of the medium and preparation were followed as described here: Dulbecco's modified Eagle's medium (DMEM) GlutaMAX 4.5 g/l glucose (#31966021) was supplemented with two sterile filtered antibiotics to prevent bacterial and fungal infections - Amphotericin B (AmpB; #15290026) and Penicillin-Streptomycin (PS, 10,000 U/mL; #15140122), plus a sterile filtered serum

to promote cell growth - fetal bovine serum (FBS; #16000044). Medium, antibiotics, and FBS were purchased from ThermoFisher Scientific (Waltham, MA, USA). When preparing the complete growth medium, 10% FBS (50 ml), 1% AmpB (5 ml), and 1% PS (5 ml) were added to the DMEM bottle (450 ml) pre-warmed at 37°C in a water bath, and the bottle was gently shaken.

A serum-free medium (SFM) - a plain DMEM GlutaMAX, i.e., a complete growth medium without FBS and antibiotics (called plain DMEM; #D6046, Sigma-Aldrich), was used for some experiments. FBS contains several growth supplements that promote cell growth and proliferation, and thus, it was advantageous to use SFM to avoid the impact of FBS when investigating other factors/chemicals that affect growth and proliferation. Similarly, the absence of antibiotics in SFM formulation was considered to avoid competition/interference of antibiotics with test substances used in the experiments.

A low glucose media – DMEM GlutaMAX 1 g/l (#21885025, ThermoFisher), was used for some experiments. When preparing the low glucose medium, 1% FBS (5 ml) was added to the DMEM bottle.

## 3.3 Cell Culturing Process

The cells were obtained from the liquid $N_2$ vapor tank and transferred to a 37°C water bath where it was thawed in a way where the sides of the vials were thawed, and the center of the vial remained frozen. 10-15 ml complete growth medium pre-warmed to 37°C were added to a 100 mm tissue culture dish (Falcon™ 353003, #10212951, Fisher Scientific), and the contents of the defrosted cell vials were poured onto the plate containing the complete growth medium. To obtain an even spread of cells, the plate was swirled gently before placing it in the incubator set at 37°C and 5% $CO_2$. Cell adherence was observed with a light microscope the next day, and the medium was changed to get rid of dead/non-adherent floating cells and the leftover components from the freezing medium. The cells were then placed in an incubator, changing the media every 3-4 days as needed until they reached sufficient confluence (>70%).

When the cells reached the desired confluency, trypsinization was performed to detach the adherent cells to either further passaging or seeding for the experiment. When trypsinizing, the growth medium was first removed from the plate as much as possible. To get rid of any remaining FBS (containing medium), which inhibits trypsin activity due to protease inhibitors, the plate was carefully washed 2-3 times with 1 ml PBS for each wash. PBS was added to the sides of the plate and swirled around, and PBS was removed. Thereafter, 500 µl of Trypsin-EDTA (0.25%, #25200056, ThermoFisher) was added directly on top of the cells before swirling the plate and placing it in the 37°C incubator for 3-5

minutes to activate the trypsin. *Trypsin* is a proteolytic enzyme that breaks down adhesion proteins that binds the cells to the plate in cell adhesion by cleaving the amino acids arginine and lysine at their C-terminal end. The ethylene diamine tetraacetic acid (EDTA) also enhances trypsin activity, removing calcium ions from the cell surface [88].

After incubation, a light microscope was used to observe whether all the cells had been detached, and the plate was hit gently against a hard surface (bench) if the cells were not detached completely. To deactivate the trypsin, 3 ml complete growth medium was added to the plate when all/most of the cells were detached. This cell mixture was mixed by pipetting up-down 3-4 times, transferred to a 15 ml sterile centrifuge tube, and centrifuged at room temperature for 3 minutes at 1500 rpm. After centrifugation, the supernatant was discarded, and a cell pellet (seen at the bottom of the tube) was disturbed using fingers by hitting the tube (from the outside, area close to the pellet). Lastly, the pellet was resuspended using the required amount of complete growth medium for cell counting and seeding for further experiments. Table 2 shows the plating volume of the different plates used in this study and the expected seeding density and number of cells at confluence.

**Table 2:** Overview of the different plate sizes/plating volumes and seeding densities.

| Plate | Size | Plating Volume | Seeding Density | Cells at Confluence |
|---|---|---|---|---|
| 96-well plate | 0.3 $cm^2$ | 100 µl | 0.01 x $10^6$ | 0.05 x $10^6$ |
| 12-well plate | 3.5 $cm^2$ | 1 ml | 0.1 x $10^6$ | 0.5 x $10^6$ |
| 100 mm dish | 60 $cm^2$ | 10-15 ml | 5 x $10^6$ | 20 x $10^6$ |

## 3.3.1 Cell Counting

Cell counting was performed using the Invitrogen Countess II automated cell counter or a hemocytometer (Bürker chamber). To use the automated cell counter, 10 µl each of cell mixture and trypan blue (#T8154, Sigma-Aldrich) were mixed in an Eppendorf tube, and 10 µl of this cells-trypan blue mixture was then applied to a disposable Countess cell counting chamber slide (#C10283, ThermoFisher), which was inserted into the cell counter to obtain the number of cells per ml.

Cells can also be counted manually using a Bürker chamber. The Bürker chamber and a coverslip were washed with 70% alcohol (ethanol) before the coverslip was attached to the hemocytometer using a water drop to activate the hydrostatic powers that kept them together. 10 µl of cell mixture (no trypan blue required) were added carefully between the Bürker chamber and coverslip. A light

microscope was then used to count the cells manually. The chamber consists of 3x3 squares separated by three lines, each containing 4x4 smaller squares. At least three big squares not located right next to each other were counted, and the average was calculated. To find the number of viable cells per ml in the original cell suspension, the average cell number obtained from the counting of big squares is multiplied by 10 000 ($10^4$) and with the dilution factor (for example, if the dilution is 1:5, the average is multiplied with 5).

## 3.4 Transient Gene Silencing using siRNA

To induce short-term silencing of targeted genes of interest, small interfering RNA (siRNA) was used. siRNA is a class of double-stranded short (21-25 nucleotides) non-coding RNAs, and it is the most commonly used RNA interference (RNAi) tool to achieve transient gene silencing [67]. In this thesis, the functional characterization of key regulators of glucose transport (GLUT1) and lactate production (LDHA), and transport (MCT4) was investigated using a siRNA-based gene silencing approach. Transfection efficiency was assessed using siGLO Green Transfection Indicator (Dharmacon, Lafayette, CO, USA; D-001630–01) based nuclear immunofluorescence staining. siRNA sequences of target genes are provided in Table 3.

**Table 3:** Overview of targeted siRNA sequences.

| Target Gene | Target Sequence |
|---|---|
| GLUT1 | 5’-GGCGGAAUUCAAUGCUGAUGAUGAA-3’ |
| | 5’-UUCAUCAUCAGCAUUGAAUUCCGCC-3’ |
| LDHA | 5’-UGUAGCAGAUUUGGCAGAGAGUAUA-3’ |
| | 5’-UAUACUCUCUGCCAAAUCUGCUACA-3’ |
| MCT4 | 5’-CCUCGCUCAUCAUGCUGAACCGCUA-3’ |
| | 5’-UAGCGGUUCAGCAUGAUGAGCGAGG-3’ |

Approximately 5000 cells/well were seeded in a 96-well plate and incubated overnight at 37°C with a complete growth medium. After incubation, the media was removed, and 90 µl of SFM was added to each well. Then, the cells were incubated at 37°C for 30 minutes to let the cells adapt to the new environment. Stealth siRNAs aimed at the silencing of three target genes were investigated, namely GLUT1 (SLC2A1; #HSS109811, ThermoFisher), MCT4 (SLC16A3, cat #HSS145028, ThermoFisher), and LDHA (#HSS106002, ThermoFisher). In addition, two controls were included, a non-targeting control (NTC; #AM4611, ThermoFisher) and a fluorescence control (siGLO Green Transfection Indicator, Horizon Discovery Biosciences Ltd. #D0016300120). A flowchart describing the siRNA gene silencing experiment is illustrated in Figure 3.1. As indicated, two tubes marked A

and B with equal volumes of respective solutions were prepared. Tube A contained the transfection reagent Lipofectamine RNAiMAX (#13778030, ThermoFisher.) diluted 1:10 in Opti-MEM (Gibco Opti-MEM Reduced Serum Medium, no phenol red; #11058021, ThermoFisher), and tube B contained stealth siRNA's (NTC, GLUT1, LDHA, MCT4, or siGLO) diluted 1:15 in Opti-MEM. The content of tube B was transferred into tube A and incubated for at least 5 minutes at room temperature to let the RNAiMAX and siRNA interact and form a complex. After incubation, 10 µl of the mix were added to the respective wells, and the plate was incubated for 48 hours at 37°C before proceeding to further experiments (for example, glucose uptake or lactate production).

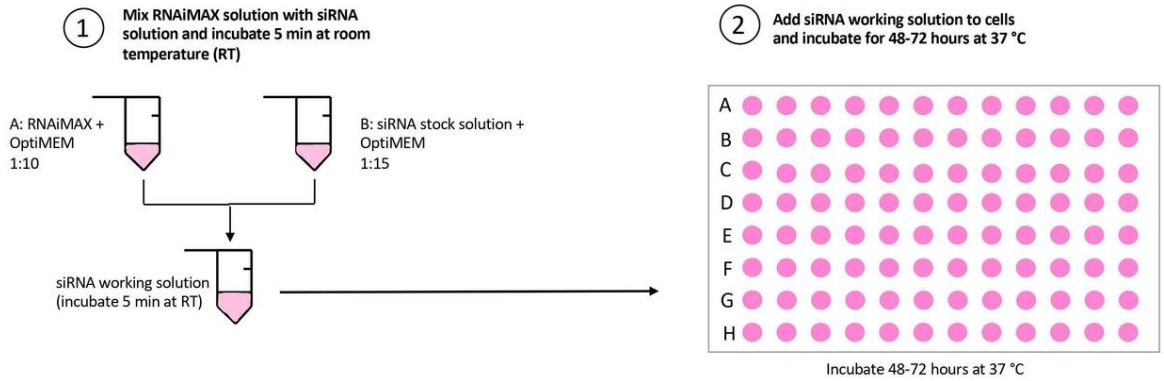


**Figure 3.1: siRNA gene silencing flowchart.** *Two tubes containing equal amounts, tube A containing the transfection reagent RNAiMAX and tube B containing siRNA, were mixed into a siRNA working solution incubated for 5 minutes at room temperature to ensure interaction between RNAiMAX and siRNA. 10 µl of the siRNA working solution was added to the cell culture wells containing 90 µl of SFM and incubated at 37°C for 48-72 hours.*

# 3.5 Expression Analysis

## 3.5.1 Immunocytochemistry

With immunocytochemistry, the presence of a specific protein or antigen can be assessed by using antibodies binding specifically to the protein/antigen of interest. In this thesis, immunocytochemistry was performed as described below to detect the expression of proteins of interest (GLUT1, LDHA, and MCT4) after transient gene silencing (using siRNA). Primary antibodies specific for each target gene produced in rabbits were used, while anti-rabbit secondary antibodies were used to recognize the bound primary antibodies.

The cells were plated in a 96-well plate with approximately 5000 cells per well and incubated overnight at 37 °C before siRNA transfection was performed. After performing siRNA transfection and incubating the cells for 48 hours at 37 °C, the media was removed and washed with 1X PBS for 5 minutes before carefully removing it. The cells were then fixated by adding 100 µl of 4%

Paraformaldehyde solution (#sc-281692, Santa Cruz Biotechnology) at 4 °C for 15 minutes. After fixation, the cells were washed with a wash buffer containing 0.1% Triton X-100 (#9002-93-1, Sigma-Aldrich) in 1X PBS three times for 3-5 minutes each time. Blocking buffer containing 5% bovine serum albumin (BSA; #A4503, Sigma-Aldrich) in 1X PBS was then added and incubated at room temperature for 1 hour. After blocking, 30 µl rabbit primary antibodies specific for GLUT1 (#SAB4200519, Sigma-Aldrich), LDHA (#3582T, Cell Signaling Technology), and MCT4 (#ab234728, Abcam) diluted 1:200 in blocking buffer were added to each well and incubated for 1 hour at room temperature (or at 4 °C overnight). Next, the cells were washed with wash buffer three times for 3-5 minutes each time before 30 µl of the secondary Alexa Fluor 594-AffiniPure Goat Anti-Rabbit IgG (#111-585-144; Jackson ImmunoResearch, UK) antibody diluted 1:200 in blocking buffer, was added to each well and incubated for 1 hour at room temperature in the dark. Next, the cells were washed three times with a wash buffer for 3-5 minutes each. The nuclei were stained by adding 30 µl DAPI (#4083S, Cell Signaling Technology) diluted 1:1000 in PBS to each well and incubated for 5-10 minutes at room temperature in the dark. The cells were then washed twice with wash buffer and once with PBS for 3-5 minutes each time. Finally, 100 µl PBS was added to each well before observing and taking pictures of the staining using the FLoid™ Cell Imaging Station (ThermoFisher Scientific).

### 3.5.2 Western Blot

Approximately 50 000 cells per well were seeded in a 12-well plate and incubated overnight at 37 °C before performing siRNA transfections. The next day, the growth medium was removed, and cells were incubated with SFM containing targeted siRNA or NTC. After 48-hour incubation at 37°C, the cell culture medium was removed, and the cells were washed with PBS. To obtain cell lysates, 100 µl Laemmli buffer containing 4% SDS, 20% glycerol, and 120 mM Tris-HCl was added to each well. Next, cell lysates were transferred to eppendorf tubes, and 2% BPB and 5% β-mercaptoethanol were added. Consequently, the samples were boiled for 5 minutes at 95°C to obtain protein extracts. Protein aliquots were separated from the protein lysates using sodium dodecyl sulfate-polyacrylamide gel electrophoresis (SDS-PAGE) with 10% polyacrylamide. A semi-dry transfer system from Bio-Rad was used to transfer the proteins to nitrocellulose membranes. The membranes were then blocked using Tris-buffered saline containing 0.1% Tween 20 (TBST) with 5% nonfat dry milk solution and incubated overnight at 4 °C with primary antibodies for GLUT1 (#SAB4200519, Sigma-Aldrich), LDHA (#3582, Cell Signaling Technology), and MCT4 (#ab234728, Abcam), as well as for the Vinculin (#13901, Cell Signaling Technology) control used to confirm equal protein loading. The next day, the blots were washed three times with TBST before being incubated with HRP-conjugated Goat Anti-Rabbit secondary antibodies (#1706515, Bio-Rad Laboratories) for 1 hour at room temperature. To process and visualize the blots, LumiGLO® (KPL, Gaithersburg, MD, USA) was used. Finally,

Labworks Software (UVP, Cambridge, UK) was used to perform the densitometric analysis of the blots.

## 3.6 MTT Cell Viability Assay

Among various assays available for the assessment of cell viability, an MTT-based cell viability assay was used in this thesis. This assay is based on the following principle: the water-soluble yellow tetrazolium salt, called thiazolyl blue tetrazolium bromide (MTT), is converted into insoluble purple formazan crystals actively respiring cells by the mitochondria. Briefly, the MTT assay measures the amount of formazan formation, which indicates the number of viable cells.

After performing siRNA gene silencing on all three target genes (GLUT1, LDHA, and MCT4) and incubating the cells for 48 hours, a mixture of MTT (#M2128, Sigma-Aldrich) labeling reagent diluted 1:20 (5 µl MTT per 100 µl) in plain DMEM (SFM), were prepared. The culture medium was removed, and 100 µl of the MTT-DMEM mix was added to each well. Then, cells were incubated at 37 °C for 4 hours. For negative control, MTT reagent was added to wells without cells. After the purple-colored formazan crystals were observed under the light microscope, the culture medium was carefully removed, and 100 µl DMSO was added to each well to solubilize the purple-colored formazan crystals. Lastly, a spectrophotometer set at 570 nm was used to read the absorbance.

## 3.7 BrdU Cell Proliferation Assay

In principle, the assay determines the amount of pyrimidine analog bromodeoxyuridine (BrdU) incorporated into the newly synthesized DNA of proliferating cells instead of thymidine. Briefly, the cells are incubated with BrdU reagent, followed by its detection using primary antibodies and horseradish peroxidase (HRP)-conjugated secondary antibodies. The signal is amplified using an HRP substrate 3,3',5,5'-tetramethylbenzidine (TMB) and detected using a spectrophotometer.

To investigate whether siRNA gene silencing affects cell proliferation, following siRNA transfections, a BrdU cell proliferation assay was performed at two different time points, 72 hours, and seven days. The "BrdU Cell Proliferation ELISA Kit (colorimetric)" (#ab126556, Abcam) was used, and all the reagents were prepared according to this kit's manual. Approximately 5000 cells/well were seeded 100 µl/well in two 96-well plates, one for each time-point, with a complete growth medium and incubated overnight at 37°C. The following day, siRNA gene silencing was performed with six replicates for each gene of interest (GLUT1, LDHA, and MCT4), as well as for NTC, and incubated at 37°C for 3 or

7 days. Notably, the proliferation was assessed in two different sets of experimental conditions - the cells were either maintained in SFM or DMEM containing 1% FBS.

Three hours prior to the assessment time-point, the media was removed, and 100 µl of BrdU reagent was diluted in SFM (3.5 µl BrdU reagent in 8 ml SFM) was added to each well and incubated for 3 hours at 37°C. The media containing the BrdU reagent was then completely removed, and 200 µl of fixing solution was added to each well and incubated for 30 minutes at room temperature. The plate was then sealed with parafilm and stored at 2-8 °C until further use. The following day, the plates were washed three times with 100 µl 1X wash buffer. After washing, 100 µl of an anti-BrdU monoclonal detector antibody were added to each well and incubated for 1 hour at room temperature. The washing step described above was repeated before and after 100 µl 1X peroxidase goat anti-mouse IgG conjugate was added and incubated at room temperature for 30 minutes. After the incubation and last washing step, the plates were entirely flooded with distilled water and carefully hit against an absorbent paper towel to dry. Lastly, 100 µl TMB peroxidase substrate was added to each well and incubated for 30 minutes in the dark at room temperature. A turquoise/blue color will be visible in the wells containing actively proliferating cells where the amount of BrdU incorporated in the proliferating cells is directly proportional to the color intensity, ranging from turquoise/blue to bright yellow. 100 µl/well of Stop Solution was added to stop the reaction before the plates were read using a spectrophotometer set at 450 nm.

# 3.8 Glucose Metabolism

Intracellular glucose transport and lactate production/secretion in the medium (a measure of glycolysis) was assessed to investigate the impact of transient silencing of GLUT1, LDHA, or MCT4 on the glycometabolic changes, as described below.

## 3.8.1 Glucose Transport

Briefly, to assess the ability of PCCs to transport glucose, cells were exposed with [$^3$H]-radiolabeled glucose for a particular duration, and intracellular levels of radiolabeled glucose were measured. In principle, the radioactive glucose, [$^3$H]-2-deoxy-D-glucose ([$^3$H]2-DG), is transported into the cells via the GLUT-transporters but is phosphorylated to prevent it from further being broken down once inside the cell. Phloretin, which is included in the stop-solution, inhibits the transport functions of the glucose transporters and can be used to obtain an exact stop time point.

First, a time-dependent glucose transport experiment with five time-points (1, 2, 4, 6, and 8 hours) was performed among PCCs at basal to find the optimal time-point for further experiments combined with siRNA gene silenced GLUT1, as described below.

After seeding 5000 cells/well in a 96-well plate and incubating overnight at 37°C, the media was replaced with SFM in the wells assigned for the longest-lasting time-point (8 hours). The cells were then incubated for 30 minutes at 37°C to adapt to the new environment before being washed once with PBS. Next, 100 µl of Krebs-Singer-Hepes (KRH)-buffer was added to each well. To make the KRH-buffer, 2.5 ml of the following stock solutions, 50 mM HEPES (#H3375, Sigma-Aldrich), 137 mM NaCl (#31434M, Sigma-Aldrich), 4.7 mM KCl (#P9541, Sigma-Aldrich), 1.85 mM $CaCl_2$ (#223506, Sigma-Aldrich), 1.3 mM $MgSO_4$ (#105886, Sigma-Aldrich), and 0.1% BSA (Sigma-Aldrich), as well as 35 ml MQ-water were added into a 50 ml tube and filtered through a 0.2 µl filter to make it sterile. 10 µl start-solution, which contains 9.395 µl PBS, 0.55 µl 2-deoxy-D-glucose stock (#D8375-1G, Sigma-Aldrich), and 0.055 µl [$^3$H]2-DG stock [#NET238C001MC, Perkin Elmer (Waltham, MA, USA)], were added to each well and incubated for 8 hours at 37°C. The procedure was repeated for each time point so that all the time points were completed simultaneously. After 8 hours, 5 µl stop-solution per well containing 3.79 µl PBS, 1 µl methanol stock (#34860, Sigma-Aldrich), and 0.21 µl phloretin stock (#P7912, Sigma-Aldrich), was added to all the wells and incubated for 10 minutes at 37 °C. After that, the media was removed, and the cells were washed with ice-cold PBS three times. The cells can be frozen down at this point or further processed to cell lysis by adding 100 µl 0.1 M sodium hydroxide (NaOH) to each well and incubating for 10 minutes at room temperature on a see-saw shaker. 50 µl of each of the samples were transferred to marked scintillation tubes before adding 4 ml of the scintillation solution Opti-Fluor (#6013199, Perkin Elmer) and mixing the tubes. Finally, the radioactive glucose inside the lysates, directly proportional to the amount of [$^3$H]2-DG taken up by the cells, was measured using a liquid scintillation counter.

After a single time-point was determined by the basal time-dependent experiment described above, it was used to investigate the difference in glucose transport between basal cells and cells transfected with siRNA against GLUT1 or NTC controls. Briefly, following the transfections, cells were incubated for 48 hours at 37 °C prior to following the same procedure as the basal experiment to assess the glucose transport at a single time-point.

### 3.8.2 Assessment of Glycolysis through Lactate Secretion

Lactate is produced and secreted by the cells during anaerobic glycolysis, which is the principle of this assay. In the medium, lactate and NAD+ are converted into pyruvate and NADH by lactate dehydrogenase (LDH). A tetrazolium salt is reduced to a colored formazan in the reaction solution by

NADH. Formazan absorbs light between 490 and 520 nm. The assay is an indirect measure of glycolysis activity because lactate in the medium is directly proportional to the amount of formazan present.

The cells were seeded at a density of 5000 cells/well in a 96-well plate and incubated overnight at 37°C before being transfected with siRNA for all three target genes (GLUT1, LDHA, or MCT4). The next day, the growth medium was replaced with plain low glucose DMEM and incubated for 48 hours at 37 °C. After 48 hours, the media was collected in separate tubes and stored at -20°C for further use.

A "Glycolysis Cell-Based Assay" kit (#600450, Cayman Chemical Ann Arbor, MI, USA) was used to perform the assay, and the manufacturer's instructions were followed to prepare reagents and perform the assay. First, the L-lactate stock (10 mM) was mixed with culture medium as the diluent to make a standard dilution range from 0 to 10 mM, as illustrated in Table 4. 90 µl of assay buffer, which is prepared by dissolving a Cell-Based Assay Buffer Tablet in 100 ml distilled water, was added to each well of a 96-well assay plate. 10 µl of standards and a blank were added in duplicates to the first two columns of the plate, and 10 µl siRNA transfected cells were added to the remaining wells. 100 µl Reaction Solution, which contains substrate, cofactor, and enzyme mixture, was added to each well before the plate was incubated on a see-saw shaker for 30 minutes at room temperature. Finally, the absorbance was read with a spectrophotometer set at 490 nm.

**Table 4:** Standard dilution range of L-lactate dilution scheme.

| Vial | Volume of Diluent (µl) | Source and Volume of L-Lactate (µl) | L-Lactate concentration (mM) |
|---|---|---|---|
| A | 0 | 300 of stock | 10 |
| B | 100 | 100 of vial A | 5 |
| C | 100 | 100 of vial B | 2.5 |
| D | 100 | 100 of vial C | 1.25 |
| E | 100 | 100 of vial D | 0.625 |
| F | 100 | 100 of vial E | 0.313 |
| G | 100 | 100 of vial F | 0.156 |
| H | 200 | 0 | 0 = Blank |

## 3.9 Assessment of Protein Concentration

Protein concentration was measured using the Bradford protein assay. The protein amount was used to account for the differences in cell numbers between the replicates. A brown color (maximum absorbance 465 nm), which indicates no bound proteins, is converted in an acidic environment into a blue color (maximum absorbance 610 nm) which indicates bound proteins due to a Coomassie dye in the Bradford reagent. The protein concentration is directly proportional to the intensity of the blue color. The Bradford protein assay is described below.

**Table 5:** Standard dilution range of BSA dilution scheme.

| Vial | Volume of Diluent (0.1 M NaOH) (µl) | Volume and Source of BSA (µl) | Final BSA Concentration (µg/ml) |
|---|---|---|---|
| A | 0 | 300 of stock | 2000 |
| B | 125 | 375 of stock | 1500 |
| C | 325 | 325 of stock | 1000 |
| D | 325 | 325 of vial C | 500 |
| E | 325 | 325 of vial E | 250 |
| F | 325 | 325 of vial F | 125 |
| G | 400 | 100 of vial G | 25 |
| H | 400 | 0 | 0 = Blank |

BSA stock (2000 µg/ml) and a diluent (0.1 M NaOH) were mixed to make a standard dilution range with known concentrations, as illustrated in Table 5. 10 µl of the standards (25, 125, 250, 500, 1000, 1500, and 2000 µg/ml), as well as a blank, were added in duplicates in the first two columns of a 96-well plate as shown in Table 6. From each sample, 20 µl were added to the remaining wells. 200 µl of Bradford reagent (Sigma-Aldrich) was added to all wells, standards, and samples. Lastly, a spectrophotometer set at 595 nm was used to read the protein concentration.

**Table 6:** Plate setup for the standards of the Bradford protein concentration assay.

| | 1 (standard | 2 (standard) | 3 | 4 | 5 | 6 | 7 | 8 | 9 | 10 | 11 | 12 |
|---|---|---|---|---|---|---|---|---|---|---|---|---|
| A | **Blank** | **Blank** | | | | | | | | | | |
| B | **25** | **25** | | | | | | | | | | |
| C | **125** | **125** | | | | | | | | | | |
| D | **250** | **250** | | | | | | | | | | |
| E | **500** | **500** | | | | | | | | | | |
| F | **1000** | **1000** | | | | | | | | | | |
| G | **1500** | **1500** | | | | | | | | | | |
| H | **2000** | **2000** | | | | | | | | | | |

## 3.10 Assessment of Response to Chemosensitivity

An MTT-based cell viability assay was used to compare PCCs at basal to PCCs transfected with siRNAs to investigate whether siRNA gene silencing of GLUT1, LDHA, and MCT4 impact PCC chemosensitivity towards gemcitabine and 5-FU. The comparison was performed at a single time-point and at a half-maximal inhibitory concentration ($IC_{50}$), a quantitative measure indicating how much of the drug is needed to inhibit a biological process or component by 50%. The procedure is described below.

The cells were seeded approximately 5000 cells/well in a 96-well plate and incubated at 37 °C overnight. Then, the cells were transfected with siRNAs and incubated overnight before the media was replaced with LG and NG media and incubated overnight. Next, the medium was replaced with 100 µl drug-containing medium for each well: 1 mM gemcitabine (#G6423, Sigma-Aldrich) and 5-FU (#F6627, Sigma-Aldrich) stock solutions were diluted in SFM to obtain a final concentration of 10 µM. The cells were further incubated at 37 °C for 96 hours. Lastly, an MTT assay (see details in section 3.5) was performed to assess the reduction in cell viability as a measure of drug-induced cytotoxicity.

## 3.11 Statistical Analysis

All values are presented as mean, and all error bars are calculated as the standard error of the mean (SEM). For comparison of two groups, a two-tailed unpaired student's t-test was used to perform statistical analysis. Statistically significant results were considered to be P-values $\leq 0.05$.

# 4 Results

## 4.1 Expression Analysis

Transient transfection using siRNA against three target genes, GLUT1, LDHA, or MCT4, was performed in three PDAC cell lines, BxPC-3, Mia PaCa-2, and Panc-1. siRNA against non-targeting control (NTC) was used for the comparison. The success of gene silencing (transfection) was assessed using expression analysis. Cells transfected with siRNAs against both target genes and NTC were incubated for 48 hours. Cells were either processed for immunocytochemistry or western blot analysis (for further details, see sections 3.5.1 and 3.5.2, respectively) to visualize the differences in the protein expression. Figure 4.1 shows the representative pictures of cells immunostained for target genes (RED color) and nuclei stained with DAPI (BLUE color).

### 4.1.1 Immunocytochemistry

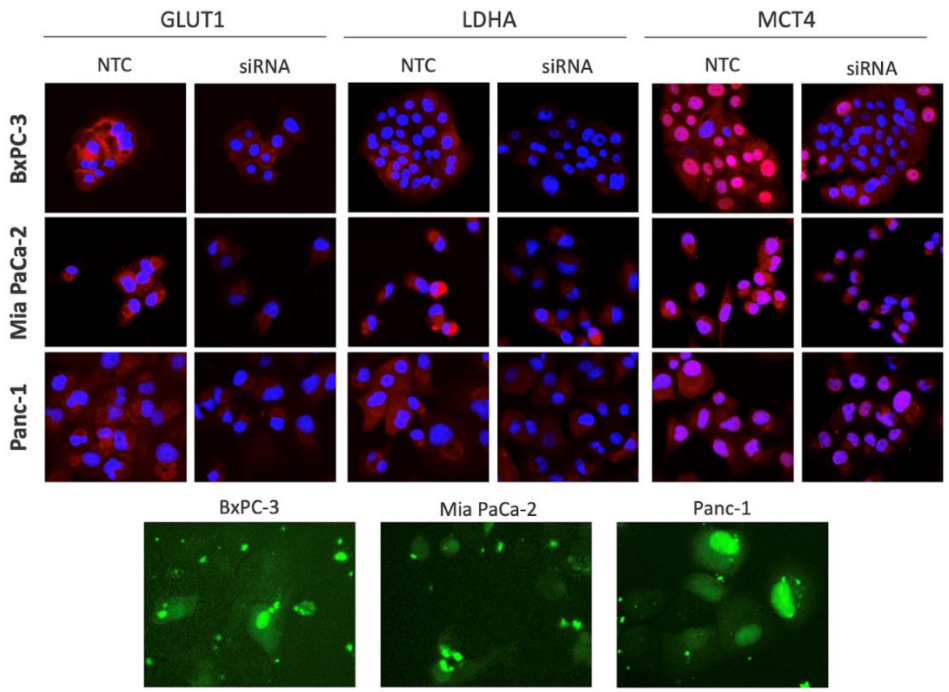


**Figure 4.1: Immunostaining.** *Three PCC lines, BxPC-3, Mia PaCa-2, and Panc-1 were seeded approximately 5000 cells/well in a 96-well plate and incubated overnight. Next, a transient transfection using NTC and targeted siRNA against GLUT1, LDHA, and MCT4, were performed and incubated at 37°C for 48 hours. The cells were then immunostained using antibodies against target genes, and pictures were captured using the FLoid Cell Imaging Station. The blue color represents the nuclei staining using DAPI, and the red color represents the positive staining for target genes. The green color represents the positive siGLO staining. NTC, non-targeting control; GLUT, glucose transporter 1; LDHA, lactate dehydrogenase A; MCT4, monocarboxylate transporter 4; DAPI, 4',6'-diamidino-2-phenylindole; siRNA, small interfering RNA.*

As shown in Figure 4.1, a positive staining of all three target genes is observed in NTC transfected cells in all three cell lines studied, although at variable levels. A significant decrease in staining intensity is observed in the cells transfected with targeted siRNA compared to NTC transfected cells. Comparing NTC and siRNA transfected cells, the GLUT1 staining shows the most significant difference, while MCT4 staining shows the least difference. The LDHA staining shows a low intensity both at basal and in cells transfected with targeted siRNA, except in BxPC-3, where basal has a significantly higher intensity. Differences between the cell lines were also observed. BxPC-3 showed an overall higher intensity in all staining, while Mia PaCa-2 and Panc-1 showed a significantly lower overall expression of GLUT1 and LDHA. However, MCT4 shows a high overall expression in all three cell lines, both at basal and in cells transfected with targeted siRNA. In addition, siGLO, used as a control for confirming the success of the transfection procedure, showed positive staining in the nucleus of at least 50% of cells in each PCC line. Of note, in line with the reported knowledge, a difference in the growth pattern between three PCC lines was observed. BxPC-3 grew in big oval lumps (colonies), Panc-1 grew in smaller rounder lumps (colonies), whereas Mia PaCa-2 grew as individual cells.

## 4.1.2 Western Blot Analysis

To further confirm the success of gene silencing, a western blot-based protein expression analysis was performed. The results are shown in Figure 4.2.

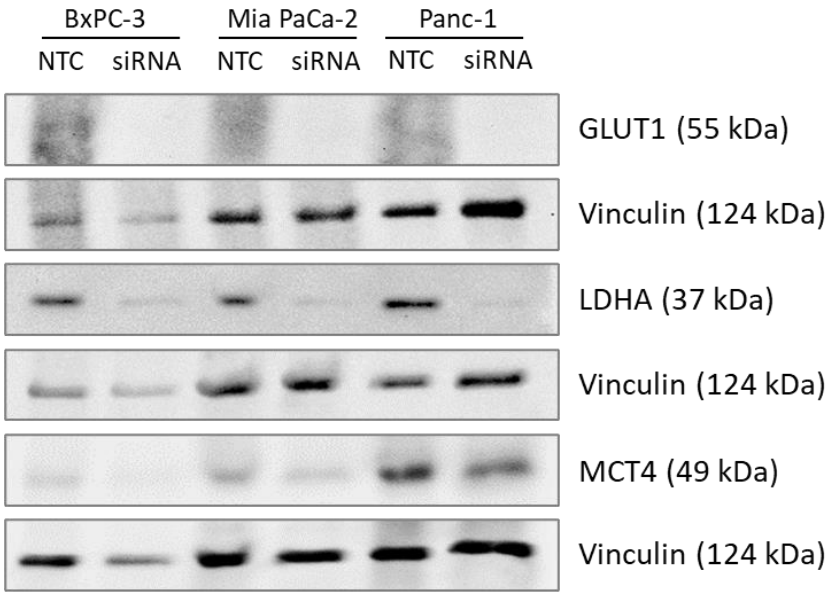


**Figure 4.2: Western blot-based protein expression analysis.** *BxPC-3, Mia PaCa-2, and Panc-1 were seeded approximately 50,000 cells/well in a 12-well plate and incubated overnight before the cells were transfected with siRNAs and NTC and incubated 48 hours. After incubation, protein lysates were obtained, proteins were separated from the lysates by SDS-PAGE, and a semi-dry transfer system was used to transfer the proteins to nitrocellulose membranes. Next, the membranes were incubated with respective primary antibodies and secondary antibodies. Lastly, LumiGLO® was used to visualize the blots, and Labworks Software was used to perform the densitometric analysis of the blots. SDS-PAGE, Sodium deodecyl sulphate-polyacrylamide gel electrophoresis; siRNA, small interfering RNA; NTC, non-targeting control; GLUT1, glucose transporter 1; LDHA, lactate dehydrogenase A; MCT4, monocarboxylate transporter 4.*

In line with the observations in the immunostaining experiment, a successful reduction in the expression of GLUT1, LDHA, and MCT4 was observed at 48 hours from the time of gene silencing. Across three PCC lines, the largest reduction in protein expression appears to be achieved in GLUT1, followed by LDHA and MCT4. No detectable differences in the level of reduction were observed between the cell lines when comparing NTC to siRNAs for both GLUT1 and LDHA. For MCT4, however, a pattern with the highest reduction in BxPC-3, followed by Mia PaCa-2 and Panc-1, was observed. The equal protein loading was confirmed using Vinculin expression. Of note, obtaining a clear band using the anti-GLUT1 antibody was difficult, and it only appears as a smear with a small visible band in the background. Anti-GLUT1 from another supplier was also tested; however, without a positive outcome.

## 4.2 Cell Viability

An MTT-based assay was used to investigate whether the silencing of the target genes affected cell viability. Before the MTT assay was performed (see details in section 3.6), the three PCC lines BxPC-3, Mia PaCa-2, and Panc-1 were transfected with siRNAs against GLUT1, LDHA, or MCT4, as well as NTC, and incubated for 48 hours at 37 °C. The cell viability is indicated by the formation of purple-colored formazan crystals converted from MTT by the mitochondria of metabolically viable cells. Figure 4.3 shows the results of the MTT assay in the form of relative cell viability compared to NTC transfected cells for whom the viability is set at 100%.

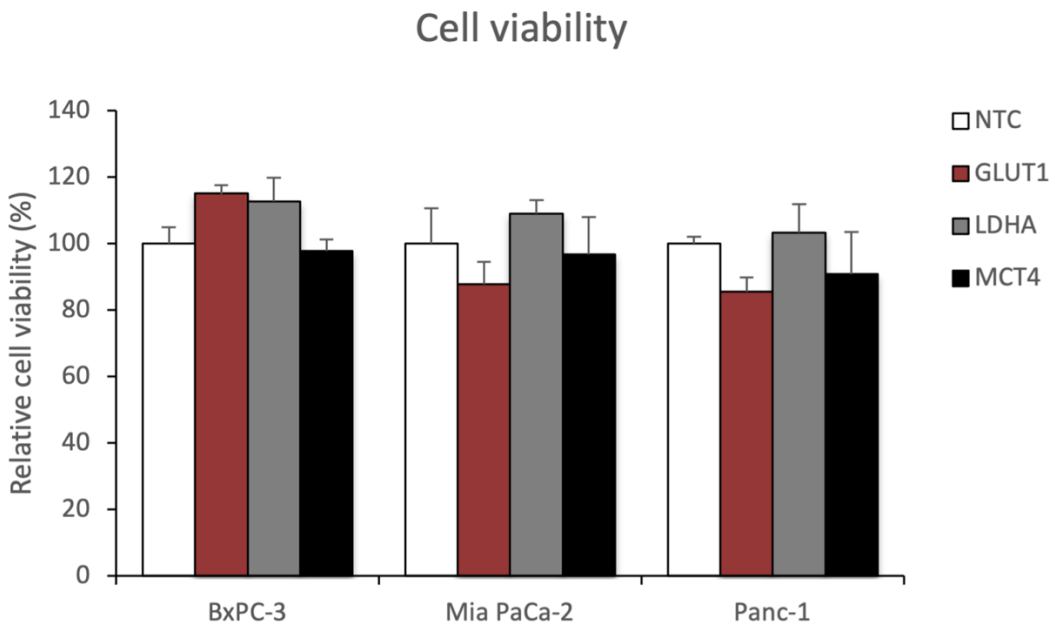


**Figure 4.3: Cell viability assessment.** *MTT assay was used to compare the cell viability at basal (NTC) with cells transfected with targeted siRNAs for GLUT1, LDHA, and MCT4. The PCC lines BxPC-3, Mia PaCa-2, and Panc-1 were seeded approximately 5000 cells/well in a 96-well plate and incubated overnight before being transfected with targeted siRNAs and NTC and were further incubated for 48 hours. An MTT assay was performed to measure cell viability, and the absorbance was read using a spectrophotometer set at 570 nm. The basal condition (NTC) was compared with the other conditions by a percentage change in the number of viable cells. The error bars are indicated by the calculated standard error of the mean (SEM). MTT, thiazolyl blue tetrazolium bromide; NTC, non-targeting control; GLUT1, glucose transporter 1; LDHA, lactate dehydrogenase A; MCT4, monocarboxylate transporter 4; siRNA, small interfering RNA, PCC, pancreatic cancer cell.*

As shown in Figure 4.3, no significant difference was seen when comparing the cell viability between cells transfected with targeted siRNAs and NTC. Silencing of LDHA showed a minor increase in the cell viability in all three PCC lines. However, it was not significant statistically, whereas silencing of MCT4 displayed no impact on viability. The silencing of GLUT1 showed variable effects between cell lines. Approximately 15% increase and decrease in viability in BxPC-3 and Panc-1, respectively,

while Mia PaCa-2 showed no significant difference in viability comparing cells transfected with NTC with GLUT1 silenced cells.

## 4.3 Cell Proliferation

After finding the impact of the targeted siRNAs on cell viability, a BrdU cell proliferation assay was performed to investigate whether the targeted siRNAs affect cell proliferation over an extended incubation period. For this purpose, BxPC-3, Mia PaCa-2, and Panc-1 were seeded approximately 5000 cells/well in a 96-well plate and incubated overnight. The transient transfection was then performed using NTC and the three targeted siRNAs - GLUT1, LDHA, or MCT4. The transfected cells were kept in culture for three and seven days, and the media was changed twice during the seven-day period. Growth medium DMEM containing 1% FBS was used to maintain the nutrition supplement and prevent cell death. After three and seven days, the BrdU assay was performed, and the absorbance was measured at 450 nm using a spectrophotometer. Figure 4.4 shows the results of the BrdU assay in the form of relative cell proliferation.

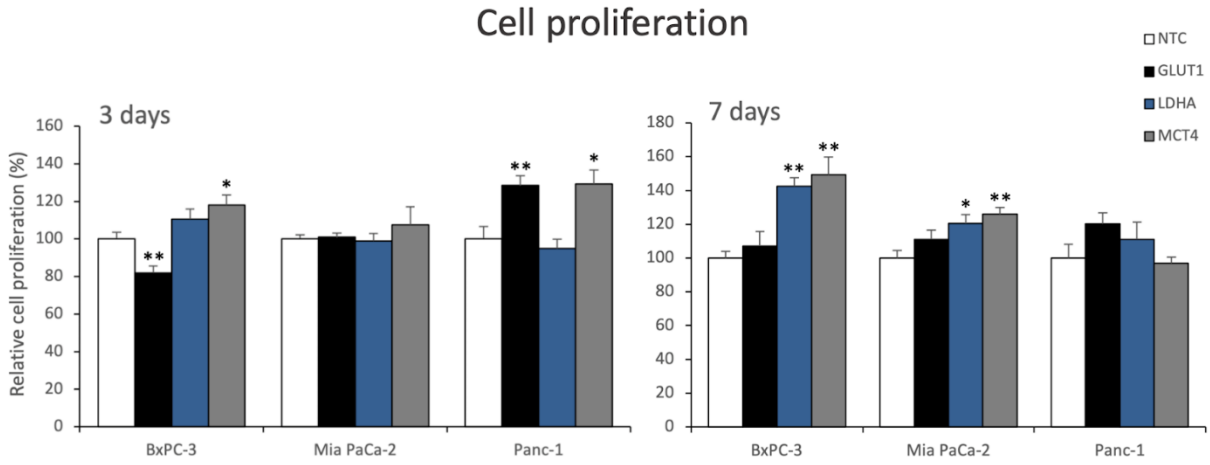


**Figure 4.4: BrdU cell proliferation assay.** *The assay was used to compare the proliferating cells transfected with NTC and targeted siRNAs - GLUT1, LDHA, and MCT4, after an incubation period of three and seven days. BxPC-3, Mia PaCa-2, and Panc-1 were seeded approximately. 5000 cells/well in a 96-well plate and were transfected with NTC or targeted siRNAs, followed by incubation with DMEM + 1% FBS for a period of three and seven days. After the incubation periods, the BrdU cell proliferation assay was performed, and the absorbance was measured using a spectrophotometer set at 450 nm. The error bars are indicated as the SEM. *p<0.05, **p<0.01 comparing NTC to GLUT1, LDHA, and MCT4. BrdU, Bromodeoxyuridine; NTC, non-targeting control; GLUT1, glucose transporter 1; LDHA, lactate dehydrogenase A; MCT4, monocarboxylate transporter 4; DMEM, Dulbecco's modified eagle medium; FBS, fetal bovine serum; siRNA, small interfering RNA; SEM, standard error of the mean.*

As shown in Figure 4.4, some variation in proliferation was observed when comparing the cells transfected with NTC to the targeted siRNAs - GLUT1, LDHA, and MCT4. The 3-day incubation showed no significant differences in Mia PaCa-2, while MCT4 silencing in BxPC-3 and the silencing of both GLUT1 and MCT4 in Panc-1 showed a significant increase in proliferation. Moreover, GLUT1 silencing in BxPC-3 showed a significant decrease in proliferation.

When looking at the 7 days incubation, the most negligible overall difference was found in cells with silenced GLUT1, with no significant difference in proliferation in any of the cell lines. However, a significant increase in proliferation in cells with silenced LDHA or MCT4 was found in BxPC-3 (40-50%) and Mia PaCa-2 (20-30%) compared to NTC transfected cells. Panc-1 showed no significant difference in proliferation when compared between NTC with LDHA or MCT4 silenced cells. In general, the most significant differences in the proliferation between NTC and targeted siRNAs transfected cells were found in BxPC-3, while Panc-1 showed no difference at 7 days.

## 4.4 Glucose Transport

The next step was to investigate the impact of GLUT1 silencing on glucose transport. [$^3$H]-labeled 2-DG was used to assess the glucose transport in the three different PDAC cell lines BxPC-3, Mia PaCa-2, and Panc-1. A time-dependent glucose transport assessment experiment was first performed in the cells at basal state. The assessment was performed using five different time points - 1, 2, 4, 6, and 8 hours to find the most suitable time point for further experiments. At basal, the PCC lines were seeded approximately 5000 cells/well and incubated overnight before treating them with [$^3$H]2-DG (see details in section 3.8.1). After finding the suitable time-point, a new glucose transport experiment was performed. The cells were seeded approximately 5000 cells/well, were first transfected with targeted GLUT1 siRNA and NTC, and incubated for 48 hours before the cells were treated with [$^3$H]2-DG only using the time-point selected from the time-curve experiment. A liquid scintillation counter was used to measure the amount of intracellular radiolabeled glucose in the cell lysates, which directly correlates to [$^3$H]2-DG taken up by the cells, as it is metabolically inactive and thus stored intracellularly as it is transported. In addition, protein concentration was measured using the Bradford protein assay for accounting for the differences in cell number (viability). Figure 4.5 shows the relative glucose transport at basal among the three cell lines compared to the first time-point.

## 4.4.1 Basal Glucose Transport

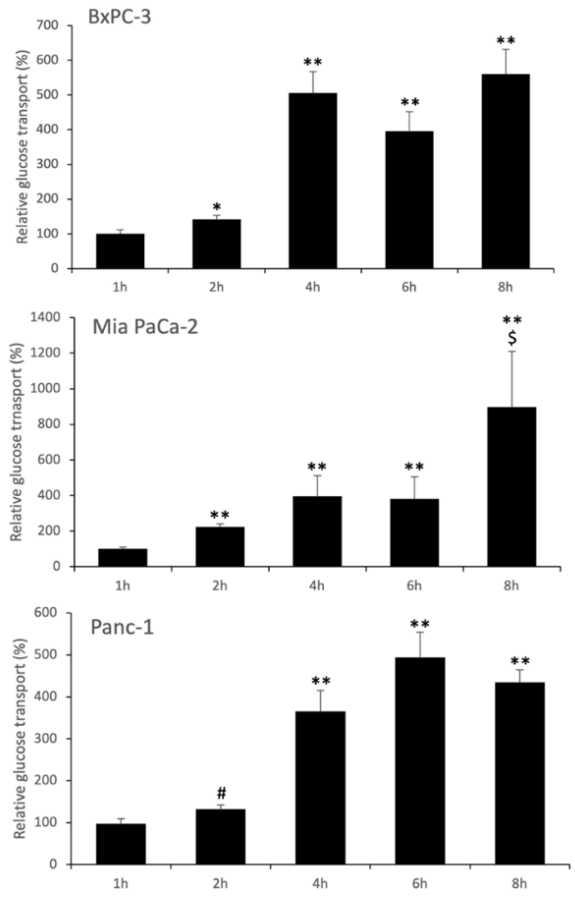


**Figure 4.5: Time-dependent glucose transport.** *Approximately 5000 cells/well were seeded of BxPC-3, Mia PaCa-2, and Panc-1 in a 96-well plate and incubated overnight. The media was replaced with SFM before the cells were incubated with [$^3$H]2-DG for 1, 2, 4, 6, and 8 hours. A liquid scintillation counter was then used to measure the ionizing radiation, and protein concentration was measured by a Bradford protein assay to justify the differences in cell number. The results are presented as a percentage change relative to the 1-hour time-point. SEM indicates the error bars. #p<01, *p<0.05, **p<0.01 comparing the glucose transport changes of 2-, 4-, 6-, and 8-hour incubations to 1-hour incubation. $p<0.05 comparing the glucose transport changes of 6- and 8-hour incubations to 4-hour incubation. SFM, serum-free DMEM; DMEM, Dulbecco's modified eagle medium; [$^3$H]2-DG, [$^3$H]-2-deoxy-D-glucose; SEM, standard error of the mean.*

As indicated in Figure 4.5, a relatively little overall change in glucose transport was observed at the 2-hour incubation compared to 1 hour. Mia PaCa-2 showed an approximately 2-fold increase in glucose transport at 2-hour, while the increase in glucose transport in BxPC-3 and Panc-1 was less than 50%. The 4-, 6-, and 8-hour incubations showed significantly higher glucose transport in all three cell lines. At 4-hour incubation, compared to 1-hour incubation, a 5-fold increase was observed at BxPC-3, while Mia PaCa-2 and Panc-1 showed an approximately 4-fold increase in glucose transport. The 6- and 8-hour incubations showed an increase between 4- and 5-fold, compared to glucose transport at 1 hour, except for the 8-hour incubation of Mia PaCa-2, which showed an almost 9-fold increase. However, there was a considerable variation between the samples at this time point. When comparing 6- and 8-hour incubations with 4-hour incubation, no significant difference in glucose transport was observed in all three cell lines, except for 8-hour incubation in Mia PaCa-2. Based on these results, a 4-hour time point was considered the point with most glucose transport and therefore was selected for future experiments.

## 4.4.2 Glucose Transport after Silencing GLUT1

Figure 4.6 shows the relative glucose transport in cells with silenced GLUT1 compared to the cells transfected with NTC, measured at a single time point of 4 hours.

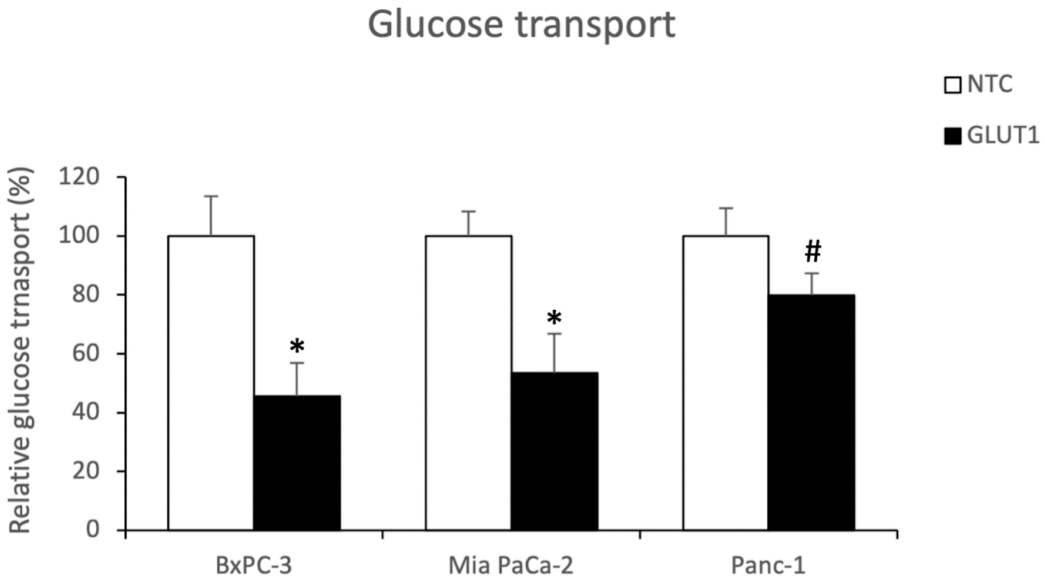


**Figure 4.6: Assessment of glucose transport.** *Three PCC lines BxPC-3, Mia PaCa-2, and Panc-1 were seeded approximately 5000 cells/well in a 96-well plate and incubated overnight before being transfected with GLUT1 siRNA and NTC. The siRNA-transfected cells were then incubated for 48 hours before being incubated with [$^3$H]2-DG for 4 hours. A percentage change comparing cells transfected with GLUT1 siRNA to NTC is used to present the results. The error bars are calculated as the SEM. #p<0.1, *p<0.05 comparing NTC to GLUT1. NTC, non-targeting control; GLUT1, glucose transporter 1; [$^3$H]2-DG, [$^3$H]-2-deoxy-D-glucose; SEM, standard error of the mean.*

As shown in Figure 4.6, a significant decrease in glucose transport in BxPC-3 and Mia PaCa-2 was observed upon GLUT1 silencing compared to NTC transfected cells. Although not statistically significant, Panc-1 showed a tendency to significance with approximately 20% decrease in glucose transport compared to GLUT1 and NTC transfected cells. The decrease in glucose transport in GLUT1 silenced cells were 55% and 50% in BxPC-3 and Mia PaCa-2, respectively, compared to NTC.

# 4.5 Lactate Secretion

To investigate the impact of the transient silencing of GLUT1, LDHA, or MCT4 on glycolysis, the amount of lactate secreted in the cell culture supernatants, a measure of glycolysis, was assessed using Glycolysis Cell-Based Assay Kit. Briefly, first, the cells were transfected with NTC or targeted siRNAs. The next day, the media was changed to low glucose DMEM and incubated for 48 hours before the supernatant was collected. Figure 4.7 shows the relative lactate secretion measured by the glycolysis cell-based assay. Results are presented comparing cells transfected with targeted siRNAs or NTC and values of NTC transfected cells set at 100%.

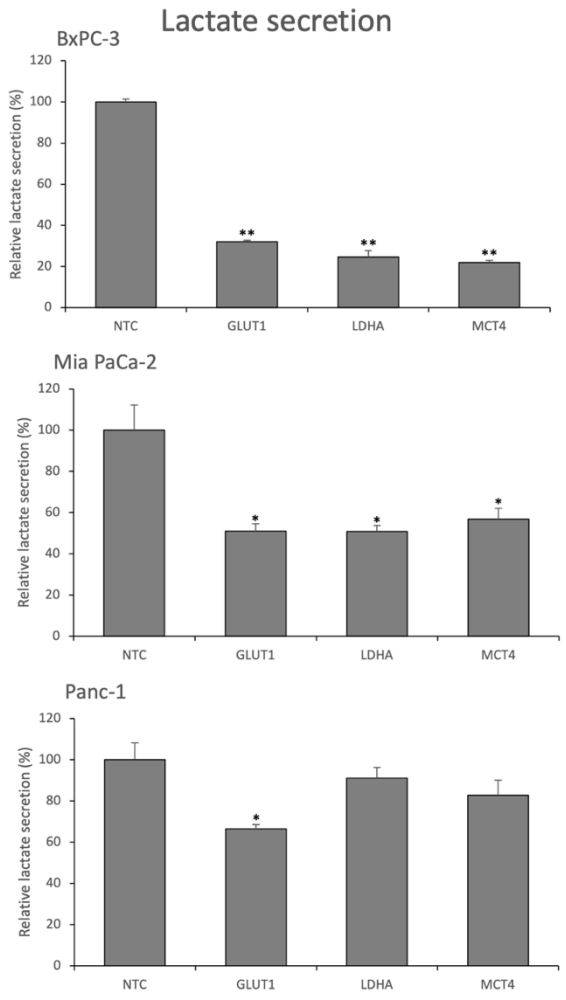


**Figure 4.7: Assessment of lactate in cell culture supernatants.** *Approximately 5000 cells/well of all three PCCs were seeded and incubated overnight before the cells were transfected with NTC and targeted siRNAs GLUT1, LDHA, and MCT4 and incubated overnight. The media was then replaced with plain low glucose DMEM and incubated for 48 hours before the cell culture supernatant was collected, and a Glycolysis Cell-Based Assay kit was used to measure lactate secretion. The result is presented as a percentage change of lactate secretion in cells transfected with GLUT1, LDHA, and MCT4 compared to NTC. The error bars are calculated as the SEM. *p<0.05, **p<0.01 comparing GLUT1, LDHA, and MCT4 to NTC. PCC, pancreatic cancer cell; NTC, non-targeting control; GLUT1, glucose transporter 1, LDHA, lactate dehydrogenase A; MCT4, monocarboxylate transporter 4, DMEM, Dulbecco's modified eagle medium; siRNA, small interfering RNA; SEM, standard error of the mean.*

As shown in Figure 4.7, an overall decrease in lactate secretion in all three PCC lines was seen when comparing cells transfected with NTC to GLUT1, LDHA, and MCT4 silenced cells. The biggest difference was observed in BxPC-3, which showed a 70-80% decrease upon silencing of all three genes. This response was relatively lower in Mia PaCa-2, which showed an approximately 50% decrease upon silencing of all three genes. In Panc-1, however, the silencing of LDHA and MCT4

showed no significant difference in lactate secretion, while the silencing of GLUT1 showed some significance with a 35% decrease in lactate secretion. The silencing of GLUT1 showed the most noticeable impact on lactate secretion, with a significant decrease in all cell lines. The lowest difference in lactate secretion, with an approximately 10% decrease, was seen upon LDHA silencing in Panc-1, although the silencing of LDHA showed a significant decrease in lactate secretion in both BxPC-3 and Mia PaCa-2.

## 4.6 Response to Chemosensitivity

The two most common chemotherapeutic agents used against PDAC are gemcitabine and 5-FU. Pancreatic tumors are known to have strong chemoresistance. However, underlying mechanisms remain unknown. Recent preliminary evidence indicates the possibility of a connection between chemoresistance and glycometabolic changes in pancreatic tumors. To this end, we investigated the impact of silencing of GLUT1, LDHA, and MCT4 on chemosensitivity of gemcitabine and 5-FU in the presence of low glucose (LG) and normal glucose (NG) conditions. Cytotoxicity was determined using the MTT-based cell viability assay. For this purpose, approximately 5000 cells/well were seeded in a 96-well plate and treated overnight. The cells were then transfected with NTC or targeted siRNAs against GLUT1, LDHA, and MCT4 and incubated overnight. After incubation, the siRNA-containing media was replaced with LG and NG-containing media before being treated with or without 10 µM gemcitabine/5-FU for 96 hours. The drug concentration was chosen based on data published previously in the laboratory. Lastly, the cytotoxicity induced by gemcitabine/5-FU was determined using an MTT assay to assess the drug-induced reduction in the cell viability.

## 4.6.1 Gemcitabine Sensitivity

Figure 4.8 shows the gemcitabine-induced cytotoxicity. The data is presented as relative cell viability in cells transfected with NTC set at 100% in cells grown in both LG and NG conditions.

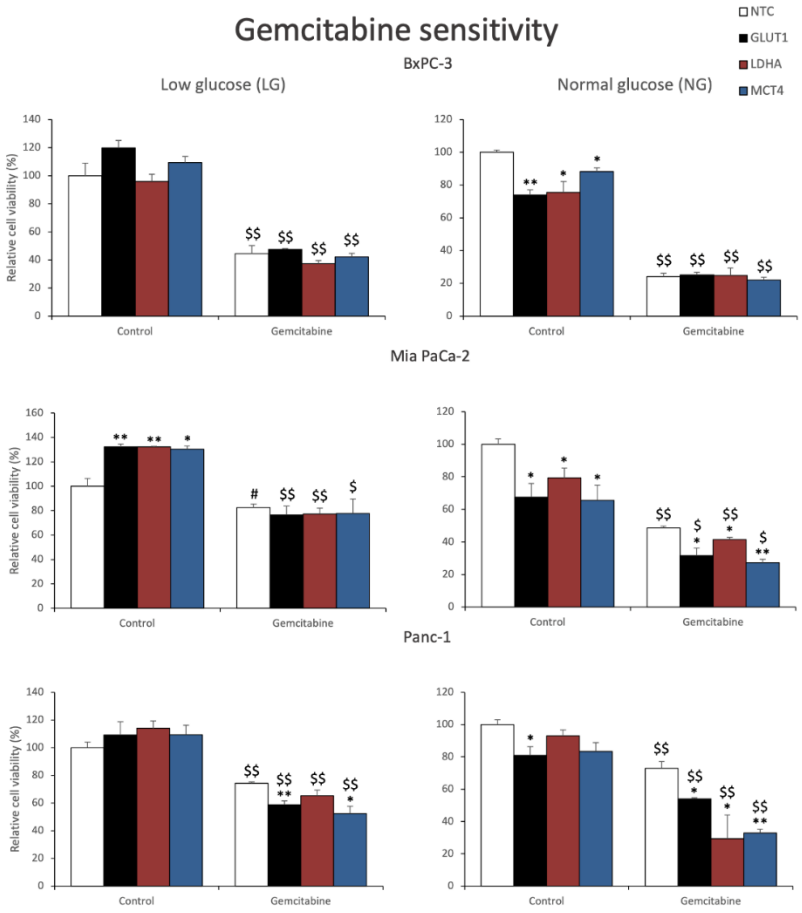


**Figure 4.8: Gemcitabine sensitivity assessment.** *Approximately 5000 cells/well of the PCCs were seeded in a 96-well plate were the cells were transfected with NTC, GLUT1, LDHA, or MCT4 siRNAs. The next day, the media was replaced with LG and NG media containing 1% FBS and incubated overnight before 10 µM gemcitabine was added to half the wells and incubated for 96 hours. After incubation, an MTT assay was performed to measure the cell viability, and the absorbance was read by a spectrophotometer set at 570 nm. The results show a percentage change comparing gemcitabine-treated siRNAs and control GLUT1, LDHA, and MCT4 to control NTC. The error bars were calculated as the SEM. *p<0.05, **p<0.01 comparing GLUT1, LDHA, and MCT4 to NTC in each condition. #p<0.1, $p<0.05, $$p<0.01 comparing untreated cells to gemcitabine-treated cells in each siRNA. PCC, pancreatic cancer cell; NTC, non-targeting control; GLUT1, glucose transporter 1; LDHA, lactate dehydrogenase A; MCT4, monocarboxylate transporter 4; LG, low glucose; NG, normal glucose; FBS, fetal bovine serum; MTT, thiazolyl blue tetrazolium bromide; SEM, standard error of the mean.*

When comparing the cells treated with 10 µM gemcitabine to the untreated cells incubated in LG media, a significant decrease in viability was seen in all cell lines (Figure 4.8). Mia PaCa-2 transfected with NTC and MCT4 siRNAs showed the smallest decrease in cell viability when comparing treated cells to untreated, but the difference was statistically significant. No significant differences in viability

were seen in BxPC-3 when comparing cells transfected with GLUT1, LDHA, and MCT4 siRNAs to NTC transfected cells in each condition separately. However, all siRNAs showed a significant increase in viability in Mia PaCa-2 control while showing no difference in gemcitabine-treated cells. For Panc-1, no significant difference in viability was observed in control cells, but the gemcitabine-treated cells showed a significant decrease in viability in GLUT1 and MCT4 silenced cells.

Cells grown in NG media also showed a significant decrease in viability in all cell lines when comparing cells treated with 10 μM gemcitabine to untreated cells, with the most negligible significant difference in viability observed in Mia PaCa-2 with silenced GLUT1 or MCT4. When comparing NTC to GLUT1, LDHA, and MCT4 in each condition separately, all siRNAs showed a significant decrease in viability in control cells in both BxPC-3 and Mia PaCa-2, while the only significant decrease in Panc-1 was observed in GLUT1. In NG condition gemcitabine-treated cells, the silencing of GLUT1, LDHA, or MCT4 compared to NTC showed no differences in viability in BxPC-3, while a minor decrease in viability was observed in Mia PaCa-2 and Panc-1.

## 4.6.2 5-Fluorouracil (5-FU) Sensitivity

Figure 4.9 shows the 5-FU-induced cytotoxicity is presented as relative cell viability in cells transfected with NTC set at 100% in cells grown in both LG and NG conditions.

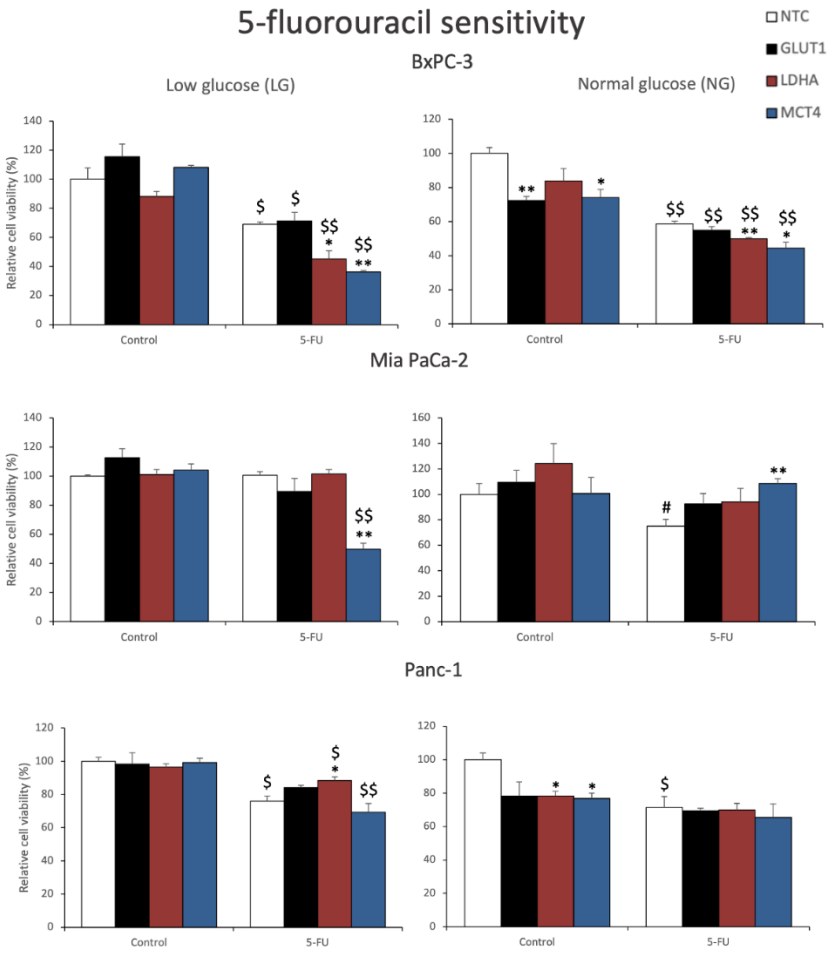


**Figure 4.9: 5-FU sensitivity assessment.** *The PCCs were seeded approximately 5000 cells/well in a 96-well plate before being transfected with NTC, GLUT1, LDHA, and MCT4 siRNAs and incubated overnight. Then, the media was replaced with LG and NG media containing 1% FBS and incubated overnight before 10 µM 5-FU was added to half the wells and incubated for 96 hours. After incubation, an MTT assay was performed to determine cell viability. Relative cell viability is presented as a percentage change comparing 5-FU-treated siRNAs and control GLUT1, LDHA, and MCT4 to control NTC. The error bars are calculated as the SEM. *p<0.05, **p<0.01 comparing NTC to GLUT1, LDHA, and MCT4 in each condition. #p<0.1, $p<0.05, $$p<0.01 comparing untreated cells to 5-FU-treated cells in each siRNA. 5-FU, 5-fluorouracil; PCC, pancreatic cancer cell; NTC, non-targeting control; GLUT1, glucose transporter 1; LDHA, lactate dehydrogenase A; MCT4, monocarboxylate transporter 4; LG, low glucose; NG, normal glucose; FBS, fetal bovine serum; MTT, thiazolyl blue tetrazolium bromide; SEM, standard error of the mean.*

When comparing cells treated with 10 µM 5-FU to untreated cells incubated in LG media, a significant decrease in viability was observed in all siRNAs in BxPC-3 and NTC, LDHA, and MCT4 in Panc-1 (Figure 4.9). In Mia PaCa-2, however, the only significant decrease in viability was seen in

MCT4 silenced cells. No significant differences in viability were observed when comparing cells transfected with GLUT1, LDHA, and MCT4 siRNAs to NTC in the control (untreated) group. LDHA and MCT4 in BxPC-3 and MCT4 in Mia PaCa-2 in 5-FU-treated cells showed a significant decrease in viability compared to NTC, while LDHA in Panc-1 showed a significant increase in viability.

In the cells incubated in NG media, all siRNAs in BxPC-3 and NTC in Mia PaCa-2 and Panc-1 showed a significant decrease in viability when comparing 5-FU-treated cells to control untreated cells. Upon silencing of GLUT1 and MCT4 in BxPC-3 and LDHA and MCT4 in Panc-1, a significant decrease in viability was observed in the control, while Mia PaCa-2 showed no differences in viability. In the 5-FU-treated cells, silencing of LDHA and MCT4 in BxPC-3 and MCT4 in Mia PaCa-2 showed a significant difference in viability when compared to NTC, while Panc-1 showed no significant differences in viability.

# 5 Discussion

The most common type of pancreatic cancer, pancreatic ductal adenocarcinoma (PDAC), is one of the most aggressive and deadliest cancer types. The 5-year survival rate is less than 10%, and 80-85% of patients are diagnosed with unresectable disease, likely due to vague and non-specific symptoms and early metastasis [12, 16]. Reprogrammed glucose metabolism, for which oncogenic KRAS is the dominant driver mutation, is one of the hallmarks of pancreatic cancer [21, 54]. Several essential metabolic proteins have been investigated as potential therapeutic targets and prognostic markers for PDAC, and this thesis focuses on three metabolic proteins that are often overexpressed in pancreatic cancer, namely GLUT1, LDHA, and MCT4 [54, 89].

Several studies have investigated the potential therapeutic target and prognostic value of GLUT1, LDHA, and MCT4 [58, 59, 61, 90]. GLUT1, one of the most crucial glucose transporters in PDAC, is a transmembrane protein that transports glucose across the hydrophobic membrane, hence it plays a key role in regulating glycolysis and other metabolic pathways linked to glucose. Overexpression of GLUT1 in PDAC contributes to enhanced glucose uptake/transport needed for malignant cell growth and is associated with treatment resistance and poor prognosis [91, 92]. LDHA is responsible for catalyzing the conversion of pyruvate to lactate, which is critical in cancer cells that are dependent on lactate production despite oxygen availability, known as the Warburg effect or aerobic glycolysis. Due to this role in providing cancer cells with lactate, elevated levels of LDHA are associated with cell proliferation, metastasis, tumor size, and a worse prognosis [54, 59]. Overexpression of MCT4 also plays a vital role in lactate production and secretion as it is one of the major lactate transporters in PDAC. The MCT-mediated transport of lactate leads to inhibition of further glycolysis due to a decrease in cytosolic pH. Upregulation of MCT4 in PDAC is associated with cancer cell growth and survival and a worse patient outcome [54, 60].

The elevated levels of GLUT1, LDHA, and MCT4 are critical for pancreatic cancer cell growth and survival, but the potential prognostic value of these metabolic proteins remains poorly understood. In recent years, their impact on chemosensitivity is also being investigated, but more research is needed before these metabolic proteins may be considered as therapeutic targets [59, 60, 91, 93]. In this study, a siRNA-based transient gene silencing approach was used to achieve a short-term temporary suppression of GLUT1, LDHA, or MCT4 expression in PCCs, such that the impact of these proteins on cell viability, proliferation, glucose transport, lactate production, and chemosensitivity could be assessed.

The success of gene silencing was confirmed using immunostaining and western blot analysis. In all three PCC lines used, immunostaining revealed decreased staining intensity in the cells transfected

with siRNAs compared to controls, that is, cells transfected with NTC (Figure 4.1). Differences in staining intensity were clearly visible in BxPC-3. However, the differences in staining intensity were less distinct in Mia PaCa-2 and Panc-1. Protein expression analysis using western blot further confirmed the reduced expression of all three target genes (GLUT1, LDHA, and MCT4) following siRNA-based gene silencing (Figure 4.2).

No significant differences in cell viability were found when comparing the cells with silenced GLUT1, LDHA, or MCT4, versus NTC using an MTT-based assay (Figure 4.3). This suggests no impact of silencing of these metabolic proteins on cell viability. Next, the impact of GLUT1, LDHA, or MCT4 silencing on cell proliferation was investigated using the BrdU incorporation assay. Surprisingly, silencing of LDHA or MCT4 resulted in increased proliferation in BxPC-3 and Mia PaCa-2 cells, but not in Panc-1 cells. In contrast, GLUT1 silencing had no impact on cell proliferation in any of the three cell lines.

The cells were incubated for three and seven days before performing the BrdU-based proliferation assay, and transient transfection using siRNAs causes a short-term silencing that is observable for up to seven days. Thus, one possible reason for the observed increase in proliferation in Mia PaCa-2 and Panc-1 could be that the silencing is no longer sustained, and cells have regained their normal growth at 7 days. Some significant variations were also observed after 3 days in BxPC-3 and Panc-1. Silencing of LDHA showed no impact on proliferation after 3 days, whereas silencing of GLUT1 or MCT4 in Panc-1 and silencing of MCT4 in BxPC-3 showed a significant increase in proliferation after 3 days. Silencing of GLUT1 in BxPC-3 showed a significant decrease in proliferation after 3 days. The three cell lines used in this study differ in both genotype and phenotype, as well as in mutational profiles, which may cause variations in growth and proliferation [86]. Thus, as none of the differences were extreme, one possible reason may be the natural variation of proliferation between the cell lines.

Measurements of glucose transport and lactate secretion were performed to investigate the impact of transient silencing of GLUT1, LDHA, or MCT4 on glucose metabolism. Firstly, a time-dependent glucose transport experiment was performed to determine the most appropriate time point. As shown in Figure 4.5, glucose transport was assessed at 2-, 4-, 6-, and 8-hour incubations, and results were compared with 1-hour incubation to find the most appropriate time-point. The 2-hour incubation did not show any significant differences compared to the 1-hour incubation, while the 4-, 6-, and 8-hour incubations showed a significant increase in glucose transport. Interestingly, maximum glucose transport was observed at 4 hours in all three cell lines, and it remained unchanged at 6- and 8-hour incubation, with the only exception of Mia PaCa-2 at 8 hours. However, considerably lower protein concentration was observed in Mia PaCa-2 at 8 hours. This may be explained by [$^3$H]2-DG-induced cytotoxicity due to increased cell death. [$^3$H]2-DG causes glucose deprivation-induced cytotoxicity in

a dose- and time-dependent manner when inhibiting glucose metabolism [94]. The time-dependent glucose transport experiment revealed that some sort of saturation in glucose transport was reached around 4 hours for all three cell lines, and the transport was not further increased in the next 4 hours. Thus, a 4-hour incubation was considered the most appropriate time-point for further experiments.

The most crucial glucose transporter in pancreatic cancer is GLUT1, a part of the facilitative transporters (GLUTs) family that enables glucose transport across a hydrophobic membrane in an ATP-independent manner. In some cases, high expression of GLUT1 is associated with a worse prognosis and treatment response of PDAC when compared to cases with low expression [91, 92]. Thus, after finding the 4-hour incubation to be the most appropriate time-point, glucose transport was investigated following only GLUT1 silencing and compared to NTC transfected cells (Figure 4.6). Both BxPC-3 and Mia PaCa-2 showed a significant decrease in glucose transport, while Panc-1 showed a tendency of lower glucose transport upon GLUT1 silencing. One possible explanation for the lower reduction in glucose transport in Panc-1 following GLUT1 silencing may be the difference in GLUT1 expression between the cell lines at baseline. Thus, if GLUT1 expression in Panc-1 is lower compared to BxPC-3 and Mia PaCa-2, the silencing will not result in the same large effect due to lower glucose transport in general. Another explanation could be insufficient silencing of GLUT1 or a potential of other GLUTs helping to maintain the glucose transport in the absence of primary transporter GLUT1. In addition, [$^{3}$H]2-DG-induced cytotoxicity may also possibly explain the lack of significant difference in glucose transport due to increased cell death in Panc-1 transfected with NTC.

The next step was to investigate the impact of GLUT1, LDHA, and MCT4 silencing on glycolysis, which was performed by measuring lactate secretion in the cell culture medium (Figure 4.7). The Warburg effect, the production of lactate regardless of oxygen availability, is one of the most common reprogrammed metabolic pathways in PDAC and produce less energy than regular glycolysis. However, the Warburg effect, also called aerobic glycolysis, supplies proliferating cancer cells with glycolytic intermediates, which fulfill their metabolic demands. MCT4 is one of the major lactate transporters (the other one being MCT1) and is often overexpressed in PDAC [50, 54]. When comparing cells transfected with siRNA against GLUT1, LDHA, or MCT4 to NTC transfected cells, a significant decrease in lactate secretion was observed in BxPC-3 and Mia PaCa-2 for all targeted siRNAs and GLUT1 in Panc-1 cells. The most pronounced decrease in lactate secretion was observed in BxPC-3. Due to the importance of MCT4 and LDHA in lactate production/transport, a significant decrease in lactate secretion was expected upon silencing of MCT4 or LDHA. However, silencing of LDHA or MCT4 in Panc-1 showed no impact on lactate secretion. Panc-1 also showed a lower reduction in glucose transport when silenced for GLUT1 (Figure 4.6). The differences in the results between the cell lines could possibly be explained by the differences in their mutational profiles or by their glycolysis ability in given low nutrient conditions. Further investigations are needed to identify

underlying mechanisms. The decrease in lactate secretion seen in cells silenced for GLUT1, LDHA, or MCT4 compared to NTC transfected cells further validate the essential role of these proteins in glycolysis.

Next, the PCCs transfected with siRNAs against GLUT1, LDHA, or MCT4, and NTC were investigated for the gemcitabine and 5-FU sensitivity in the presence of LG and NG conditions using an MTT assay. For more than two decades, gemcitabine has been the most commonly used cytotoxic agent for PDAC treatment. However, within weeks of treatment initiation, tumors develop drug resistance, which remains a major hurdle in achieving better treatment outcomes [77]. All three PCC lines showed a significant reduction in cell viability (caused by drug-induced cytotoxicity) upon exposure to gemcitabine in both LG and NG conditions (Figure 4.8). Comparing control with gemcitabine-treated NTC transfected cells revealed that BxPC-3 cells are most sensitive, followed by Mia PaCa-2 and Panc-1. Cytotoxic response of gemcitabine was not affected by the silencing of GLUT1, LDHA, or MCT4 in BxPC-3 and Mia PaCa-2 in LG condition and BxPC-3 in NG condition. However, interestingly, in the LG condition, silencing of GLUT1 or MCT4 in Panc-1 showed an increase in gemcitabine-induced cytotoxicity.

Similarly, Mia PaCa-2 and Panc-1 in the NG condition showed an increase in gemcitabine-induced cytotoxicity upon silencing of any of the three glycometabolic genes. Of note, a trend towards reduced viability following the silencing of GLUT1, LDHA, or MCT4, compared to NTC, was seen in all three PCC lines in the control cells in the NG condition. In contrast, the viability experiment shown in Figure 4.3 was performed in NG conditions and showed no impact on viability in any of the siRNAs. This could be partly explained by the fact that the time at which cell viability was measured differed between both experiments (48 and 96 hours for the experiment shown in Figures 4.3 and 4.8, respectively).

Furthermore, in NG conditions, gemcitabine-treated BxPC-3 cells showed no differences in viability following silencing of GLUT1, LDHA, or MCT4 compared to NTC, while a minor decrease was observed in Mia PaCa-2 and Panc-1. The differences in gemcitabine sensitivity when comparing siRNAs to NTC and between the cell lines may be partially explained by the different mutation profiles of the cell lines, particularly KRAS mutations. Oncogenic KRAS is known to play an essential role in reprogramming glucose metabolism [21, 54]. BxPC-3 contains wild-type KRAS, while Mia PaCa-2 and Panc-1 have different KRAS mutations, which may impact the expression patterns and the activity of GLUT1, LDHA, and MCT4. However, more investigations are needed to confirm whether the differences are KRAS-mediated.

The other important cytotoxic agent used against PDAC investigated in this study was 5-FU. Interestingly, the 5-FU induced reduction in cell viability in the NTC transfected cells were clearly visible in both LG and NG for BxPC-3 and Panc-1. However, Mia PaCa-2 did not show any clearly visible cytotoxicity. Silencing of GLUT1, LDHA, or MCT4 showed no impact on viability in the control, untreated cells for all three cell lines in LG, and only in Mia PaCa-2 under NG conditions (Figure 4.9). Similar to the gemcitabine sensitivity experiment (Figure 4.8), a decrease in cell viability was seen in BxPC-3 and Panc-1 cells in NG conditions when compared between siRNA and NTC. Comparing control and 5-FU treated cells revealed that the silencing of only MCT4 further increased the 5-FU sensitivity in the LG condition. However, it was not the case for either GLUT1, LDHA, or MCT4 in the NG condition. This suggests that reducing the expression of MCT4 in nutrient-poor conditions, such as in pancreatic cancer, may increase the cytotoxic response of 5-FU. Further investigations using the inhibitors of MCT4 may provide additional insights into this.

To summarize, a general trend of reduced glucose transport and lactate secretion and unchanged or improved (in some cases) chemosensitivity was observed when comparing PCCs following silencing of GLUT1, LDHA, or MCT4 to NTC transfected cells. Silenced GLUT1, LDHA, or MCT4 showed discrete or nonsignificant differences in viability and proliferation when compared to NTC transfected cells. In particular, MCT4 silencing had a significant impact on both gemcitabine and 5-FU sensitivity in all cell lines. Thus, this study provides further evidence regarding the impact of GLUT1, LDHA, and MCT4 on glycometabolic regulation and chemosensitivity in pancreatic cancer. Furthermore, significant differences between the cell lines support the well-known hallmark of pancreatic cancer - the tumor heterogeneity. In addition, the study forms the basis for further investigations into the possibility of balancing the tumor glycometabolic phenotype in an attempt to obtain better treatment outcomes.

Some of the notable limitations of this study include the lack of cell lines with stable gene silencing or long-term silencing and variations in phenotype and genotype between the cell lines. Moreover, the experiments were performed in pure cancer cell cultures, which significantly differ from the actual tumor environment, composed of a large amount of stroma. Its interaction with cancer cells is known to affect their behavior multi-dimensionally. For further research, it would be useful to include an overexpression experiment to validate the impact of selected glycometabolic proteins on glucose transport, glycolysis, and chemosensitivity. Moreover, investigating the glycolysis inhibitors in combination with chemotherapeutics agents would be worthwhile.

# 6 Conclusion

In conclusion, successful silencing of the key glycometabolic regulators GLUT1, LDHA, and MCT4 was achieved through siRNA-mediated transient transfections. This study provides preliminary evidence of a general trend towards decreased glucose transport, lactate secretion, and unaltered or improved chemosensitivity following silencing of GLUT1, LDHA, or MCT4 as compared to NTC transfected cells. Silencing of MCT4 further enhanced gemcitabine- and 5-FU-induced cytotoxicity in some conditions suggesting its essential role in regulating both glucose metabolism and chemosensitivity. This study provides further evidence of glycometabolic regulation in PDAC as a potential therapeutic target, however, further investigations are needed. Significant differences between the three PCC lines used in this study further confirm the challenge posed by heterogeneity when treating pancreatic cancer. Further investigations into the mechanisms underlying the changes induced by the silencing of GLUT1, LDHA, or MCT4 are warranted in order to better understand their therapeutic potential in pancreatic cancer treatment.

# References


1. Leung, P.S., *Overview of the pancreas.* The Renin-Angiotensin System: Current Research Progress in The Pancreas, 2010: p. 3-12.
2. Longnecker, D.S., *Anatomy and Histology of the Pancreas (version 1.0).* Pancreapedia: The Exocrine Pancreas Knowledge Base, 2014.
3. Sand, O., *Menneskets fysiologi*. 2 ed. 2014, Oslo: Gyldendal forlag AS. 872.
4. Zhou, Q. and D.A. Melton, *Pancreas regeneration.* Nature, 2018. **557**(7705): p. 351-358.
5. Pandol, S., *Pancreatic Embryology and Development.* The Exocrine Pancreas. San Rafael (CA): Morgan & Claypool Life Sciences, 2010.
6. Shyr, D. and Q. Liu, *Next generation sequencing in cancer research and clinical application.* Biological procedures online, 2013. **15**(1): p. 1-11.
7. Weinberg, R.A., *The biology of cancer*. 2 ed. 2014, New York: Garland Publishing Inc. 876.
8. Kleeff, J., et al., *Pancreatic cancer.* Nature reviews Disease primers, 2016. **2**(1): p. 1-22.
9. Wyant, T. *What Is Pancreatic Cancer?* 2019; Available from: https://www.cancer.org/cancer/pancreatic-cancer/about/what-is-pancreatic-cancer.html.
10. Vareedayah, A.A., S. Alkaade, and J.R. Taylor, *Pancreatic adenocarcinoma.* Missouri medicine, 2018. **115**(3): p. 230.
11. Sung, H., et al., *Global cancer statistics 2020: GLOBOCAN estimates of incidence and mortality worldwide for 36 cancers in 185 countries.* CA: a cancer journal for clinicians, 2021. **71**(3): p. 209-249.
12. Orth, M., et al., *Pancreatic ductal adenocarcinoma: Biological hallmarks, current status, and future perspectives of combined modality treatment approaches.* Radiation Oncology, 2019. **14**(1): p. 1-20.
13. J Ferlay, E.M., F Lam, M Colombet, L Mery, M Piñeros, A Znaor, I Soerjomataram, F Bray. *Global Cancer Observatory: Cancer Today*. 2020; Available from: https://gco.iarc.fr/today.
14. Rahib, L., et al., *Projecting cancer incidence and deaths to 2030: the unexpected burden of thyroid, liver, and pancreas cancers in the United States.* Cancer research, 2014. **74**(11): p. 2913-2921.
15. Haneborg, M.N. *Kvalitetsregister for pankreaskreft*. 2021; Available from: https://www.kreftregisteret.no/Registrene/Kvalitetsregistrene/kvalitetsregister-for-pankreaskreft/.
16. Mizrahi, J.D., et al., *Pancreatic cancer.* The Lancet, 2020. **395**(10242): p. 2008-2020.
17. Rawla, P., T. Sunkara, and V. Gaduputi, *Epidemiology of pancreatic cancer: global trends, etiology and risk factors.* World journal of oncology, 2019. **10**(1): p. 10.
18. McGuigan, A., et al., *Pancreatic cancer: A review of clinical diagnosis, epidemiology, treatment and outcomes.* World journal of gastroenterology, 2018. **24**(43): p. 4846.
19. Cicenas, J., et al., *KRAS, TP53, CDKN2A, SMAD4, BRCA1, and BRCA2 mutations in pancreatic cancer.* Cancers, 2017. **9**(5): p. 42.
20. Zeitouni, D., et al., *KRAS mutant pancreatic cancer: no lone path to an effective treatment.* Cancers, 2016. **8**(4): p. 45.
21. Waters, A.M. and C.J. Der, *KRAS: the critical driver and therapeutic target for pancreatic cancer.* Cold Spring Harbor perspectives in medicine, 2018. **8**(9): p. a031435.

22. Dardare, J., et al., *SMAD4 and the TGFβ pathway in patients with pancreatic ductal adenocarcinoma.* International journal of molecular sciences, 2020. **21**(10): p. 3534.
23. Kreftforeningen. *Bukspyttkjertelkreft*. 2022; Available from: https://kreftforeningen.no/om-kreft/kreftformer/bukspyttkjertelkreft/.
24. Adamska, A., A. Domenichini, and M. Falasca, *Pancreatic ductal adenocarcinoma: current and evolving therapies.* International journal of molecular sciences, 2017. **18**(7): p. 1338.
25. Pusceddu, S., et al., *Comparative effectiveness of gemcitabine plus nab-paclitaxel and FOLFIRINOX in the first-line setting of metastatic pancreatic cancer: a systematic review and meta-analysis*. Cancers, 2019. **11**(4): p. 484.
26. Christenson, E.S., E. Jaffee, and N.S. Azad, *Current and emerging therapies for patients with advanced pancreatic ductal adenocarcinoma: a bright future.* The Lancet Oncology, 2020. **21**(3): p. e135-e145.
27. Yao, W., A. Maitra, and H. Ying, *Recent insights into the biology of pancreatic cancer.* EBioMedicine, 2020. **53**: p. 102655.
28. Kleeff, J., et al., *Pancreatic cancer microenvironment.* International journal of cancer, 2007. **121**(4): p. 699-705.
29. Feig, C., et al., *The pancreas cancer microenvironment.* Clinical cancer research, 2012. **18**(16): p. 4266-4276.
30. Weniger, M., K.C. Honselmann, and A.S. Liss, *The extracellular matrix and pancreatic cancer: a complex relationship.* Cancers, 2018. **10**(9): p. 316.
31. Hosein, A.N., R.A. Brekken, and A. Maitra, *Pancreatic cancer stroma: an update on therapeutic targeting strategies.* Nature Reviews Gastroenterology & Hepatology, 2020. **17**(8): p. 487-505.
32. Hessmann, E., et al., *Microenvironmental determinants of pancreatic cancer.* Physiological reviews, 2020. **100**(4): p. 1707-1751.
33. Ho, W.J., E.M. Jaffee, and L. Zheng, *The tumour microenvironment in pancreatic cancer—Clinical challenges and opportunities.* Nature reviews Clinical oncology, 2020. **17**(9): p. 527-540.
34. Elyada, E., et al., *Cross-species single-cell analysis of pancreatic ductal adenocarcinoma reveals antigen-presenting cancer-associated fibroblasts.* Cancer discovery, 2019. **9**(8): p. 1102-1123.
35. Patil, K., et al., *The plasticity of pancreatic cancer stem cells: Implications in therapeutic resistance.* Cancer and Metastasis Reviews, 2021. **40**(3): p. 691-720.
36. Sunami, Y., J. Häußler, and J. Kleeff, *Cellular heterogeneity of pancreatic stellate cells, mesenchymal stem cells, and cancer-associated fibroblasts in pancreatic cancer.* Cancers, 2020. **12**(12): p. 3770.
37. Dougan, S.K., *The pancreatic cancer microenvironment.* The Cancer Journal, 2017. **23**(6): p. 321-325.
38. Cros, J., et al., *Tumor heterogeneity in pancreatic adenocarcinoma.* Pathobiology, 2018. **85**(1-2): p. 64-71.
39. Erkan, M., et al., *The activated stroma index is a novel and independent prognostic marker in pancreatic ductal adenocarcinoma.* Clinical gastroenterology and hepatology, 2008. **6**(10): p. 1155-1161.
40. Verbeke, C., *Morphological heterogeneity in ductal adenocarcinoma of the pancreas–Does it matter?* Pancreatology, 2016. **16**(3): p. 295-301.
41. Amrutkar, M., et al., *Establishment and characterization of paired primary cultures of human pancreatic cancer cells and stellate cells derived from the same tumor.* Cells, 2020. **9**(1): p. 227.

42. Ferdek, P.E. and M.A. Jakubowska, *Biology of pancreatic stellate cells—more than just pancreatic cancer*. Pflügers Archiv-European Journal of Physiology, 2017. **469**(9): p. 1039-1050.
43. Thomas, D. and P. Radhakrishnan, *Pancreatic stellate cells: the key orchestrator of the pancreatic tumor microenvironment.* Tumor Microenvironment, 2020: p. 57-70.
44. Judge, A. and M.S. Dodd, *Metabolism.* Essays Biochem, 2020. **64**(4): p. 607-647.
45. Chaudhry, R. and M. Varacallo, *Biochemistry, Glycolysis*, in *StatPearls*. 2022: Treasure Island (FL).
46. Harvey Lodish, A.B., Chris A. Kaiser, Monty Krieger, Anthony Bretscher, Hidde Ploegh, Angelika Amon, Kelsey C. Martin, *Molecular Cell Biology*. 8 ed. 2016, New York: W.H. Freeman and Company. 1280.
47. de Nava, A.S.L. and A. Raja, *Physiology, Metabolism*, in *StatPearls [Internet]*. 2021, StatPearls Publishing.
48. Chandel, N.S., *Glycolysis.* Cold Spring Harbor Perspectives in Biology, 2021. **13**(5): p. a040535.
49. Martínez-Reyes, I. and N.S. Chandel, *Mitochondrial TCA cycle metabolites control physiology and disease.* Nature communications, 2020. **11**(1): p. 1-11.
50. DeBerardinis, R.J. and N.S. Chandel, *Fundamentals of cancer metabolism.* Science advances, 2016. **2**(5): p. e1600200.
51. Melkonian, E.A. and M.P. Schury, *Biochemistry, anaerobic glycolysis.* 2019.
52. Pavlova, N.N. and C.B. Thompson, *The emerging hallmarks of cancer metabolism.* Cell metabolism, 2016. **23**(1): p. 27-47.
53. Cairns, R.A., I.S. Harris, and T.W. Mak, *Regulation of cancer cell metabolism.* Nature Reviews Cancer, 2011. **11**(2): p. 85-95.
54. Yan, L., et al., *Glucose Metabolism in Pancreatic Cancer.* Cancers (Basel), 2019. **11**(10).
55. Perera, R.M. and N. Bardeesy, *Pancreatic Cancer Metabolism: Breaking It Down to Build It Back Up.* Cancer Discov, 2015. **5**(12): p. 1247-61.
56. Nagarajan, A., et al., *Paraoxonase 2 Facilitates Pancreatic Cancer Growth and Metastasis by Stimulating GLUT1-Mediated Glucose Transport.* Mol Cell, 2017. **67**(4): p. 685-701 e6.
57. Manco, G., E. Porzio, and T.M. Carusone, *Human Paraoxonase-2 (PON2): Protein Functions and Modulation.* Antioxidants (Basel), 2021. **10**(2).
58. Yu, M., et al., *The prognostic value of GLUT1 in cancers: a systematic review and meta-analysis.* Oncotarget, 2017. **8**(26): p. 43356-43367.
59. Cui, X.G., et al., *HIF1/2alpha mediates hypoxia-induced LDHA expression in human pancreatic cancer cells.* Oncotarget, 2017. **8**(15): p. 24840-24852.
60. Baek, G., et al., *MCT4 defines a glycolytic subtype of pancreatic cancer with poor prognosis and unique metabolic dependencies.* Cell Rep, 2014. **9**(6): p. 2233-49.
61. Lee, S.H., et al., *MCT4 as a potential therapeutic target to augment gemcitabine chemosensitivity in resected pancreatic cancer.* Cell Oncol (Dordr), 2021. **44**(6): p. 1363-1371.
62. Crick, F., *Central dogma of molecular biology.* Nature, 1970. **227**(5258): p. 561-563.
63. Moriya, H., *Quantitative nature of overexpression experiments.* Molecular biology of the cell, 2015. **26**(22): p. 3932-3939.
64. Prelich, G., *Gene overexpression: uses, mechanisms, and interpretation.* Genetics, 2012. **190**(3): p. 841-854.
65. W. Filipowicz, J.P., *Brenner's Encyclopedia of Genetics*. 2 ed. Gene Silencing. Vol. 3. 2013.

66. Moazed, D., *Common themes in mechanisms of gene silencing.* Molecular cell, 2001. **8**(3): p. 489-498.
67. ThermoFisher. *Introduction to Transfection*. Available from: https://www.thermofisher.com/no/en/home/references/gibco-cell-culture-basics/transfection-basics/introduction-to-transfection.html
68. CellTransfection. *Transient versus Stable Transfection*. Available from: http://www.cell-transfection.com/cell-transfection-wiki/transient-versus-stable-transfection/.
69. ThermoFisher. *Stable Transfection*. Available from: https://www.thermofisher.com/no/en/home/references/gibco-cell-culture-basics/transfection-basics/transfection-methods/stable-transfection.html.
70. ThermoFisher. *Transient Transfection*. Available from: https://www.thermofisher.com/no/en/home/references/gibco-cell-culture-basics/transfection-basics/transfection-methods/transient-transfection.html.
71. Horizon. *siRNA Applications*. Available from: https://horizondiscovery.com/en/applications/rnai/sirna-applications.
72. ThermoFisher. *RNA interference (RNAi) Gene Specific Silencing*. Available from: https://www.thermofisher.com/no/en/home/references/ambion-tech-support/rnai-sirna/tech-notes/gene-specific-silencing-by-rnai.html.
73. McManus, M.T. and P.A. Sharp, *Gene silencing in mammals by small interfering RNAs.* Nature reviews genetics, 2002. **3**(10): p. 737-747.
74. Amrutkar, M. and I.P. Gladhaug, *Pancreatic cancer chemoresistance to gemcitabine.* Cancers, 2017. **9**(11): p. 157.
75. de Sousa Cavalcante, L. and G. Monteiro, *Gemcitabine: metabolism and molecular mechanisms of action, sensitivity and chemoresistance in pancreatic cancer.* European journal of pharmacology, 2014. **741**: p. 8-16.
76. Mini, E., et al., *Cellular pharmacology of gemcitabine.* Annals of oncology, 2006. **17**: p. v7-v12.
77. Binenbaum, Y., S. Na'ara, and Z. Gil, *Gemcitabine resistance in pancreatic ductal adenocarcinoma.* Drug Resistance Updates, 2015. **23**: p. 55-68.
78. Shukla, S.K., et al., *MUC1 and HIF-1alpha signaling crosstalk induces anabolic glucose metabolism to impart gemcitabine resistance to pancreatic cancer.* Cancer cell, 2017. **32**(1): p. 71-87. e7.
79. Rautio, J., et al., *The expanding role of prodrugs in contemporary drug design and development.* Nature Reviews Drug Discovery, 2018. **17**(8): p. 559-587.
80. Andersson, R., et al., *Gemcitabine chemoresistance in pancreatic cancer: molecular mechanisms and potential solutions.* Scandinavian journal of gastroenterology, 2009. **44**(7): p. 782-786.
81. Wang, W.-B., et al., *Recent studies of 5-fluorouracil resistance in pancreatic cancer.* World journal of gastroenterology: WJG, 2014. **20**(42): p. 15682.
82. Longley, D.B., D.P. Harkin, and P.G. Johnston, *5-fluorouracil: mechanisms of action and clinical strategies.* Nature reviews cancer, 2003. **3**(5): p. 330-338.
83. Miura, K., et al., *5-fu metabolism in cancer and orally-administrable 5-fu drugs.* Cancers, 2010. **2**(3): p. 1717-1730.
84. Mader, R.M., M. Müller, and G.G. Steger, *Resistance to 5-fluorouracil.* General Pharmacology: The Vascular System, 1998. **31**(5): p. 661-666.
85. Zhang, N., et al., *5-Fluorouracil: mechanisms of resistance and reversal strategies.* Molecules, 2008. **13**(8): p. 1551-1569.
86. Deer, E.L., et al., *Phenotype and genotype of pancreatic cancer cell lines.* Pancreas, 2010. **39**(4): p. 425.

87. ATCC. 2022; Available from: https://www.atcc.org/?geo_country=no.
88. Sigma-Aldrich. *Trypsin-EDTA solution*. 2022; Available from: https://www.sigmaaldrich.com/NO/en/product/sigma/t4049.
89. Qin, C., et al., *Metabolism of pancreatic cancer: Paving the way to better anticancer strategies.* Molecular cancer, 2020. **19**(1): p. 1-19.
90. Lyshchik, A., et al., *Expression of glucose transporter-1, hexokinase-II, proliferating cell nuclear antigen and survival of patients with pancreatic cancer.* Cancer investigation, 2007. **25**(3): p. 154-162.
91. Kurahara, H., et al., *Significance of glucose transporter type 1 (GLUT-1) expression in the therapeutic strategy for pancreatic ductal adenocarcinoma.* Annals of surgical oncology, 2018. **25**(5): p. 1432-1439.
92. Basturk, O., et al., *GLUT-1 expression in pancreatic neoplasia: implications in pathogenesis, diagnosis, and prognosis.* Pancreas, 2011. **40**(2): p. 187-92.
93. Yu, M., et al., *Metabolic phenotypes in pancreatic cancer.* PLoS One, 2015. **10**(2): p. e0115153.
94. Coleman, M.C., et al., *2-deoxy-D-glucose causes cytotoxicity, oxidative stress, and radiosensitization in pancreatic cancer.* Free Radical Biology and Medicine, 2008. **44**(3): p. 322-331.

# Appendix

## Abbreviations

| | |
|---|---|
| [$^3$H]2-DG | [$^3$H]-2-deoxy-D-glucose |
| 5-FU | 5-Fluorouracil |
| ACTA2 | Actin α-2 smooth muscle aorta |
| ADP | Adenosine diphosphate |
| AKT | Protein kinase B |
| AmpB | Amphotericin B |
| apCAF | Antigen-presenting cancer-associated fibroblast |
| ATCC | American Type Culture Collection |
| ATM | Ataxia telangiectasia mutated |
| ATP | Adenosine triphosphate |
| BRCA1 | Breast Cancer Gene 1 |
| BRCA2 | Breast Cancer Gene 2 |
| BrdU | Bromodeoxyuridine |
| BSA | Bovine serum albumin |
| CA19-9 | Cancer antigen 19-9 |
| $CaCl_2$ | Calcium chloride |
| CAF | Cancer-associated fibroblast |
| CCL | Chemokine C-C motif ligand |
| CD4 | Cluster of differentiation 4 |
| CDA | Cytidine deaminase |
| $CH_2THF$ | 5,10-methylene tetrahydrofolate |
| CDK | Cyclin-dependent kinase |
| CDKN2A | Cyclin-dependent kinase inhibitor 2A |
| $CO_2$ | Carbon dioxide |
| CoA | Coenzyme A |
| COL1A1 | Collagen type I alpha 1 chain |
| COL5A1 | Collagen type V alpha 1 chain |
| COL6A1 | Collagen type VI alpha 1 chain |
| CT | Computed tomography |
| CTGF | Connective tissue growth factor |

| | |
|---|---|
| CXCL12 | C-X-C motif chemokine 12 |
| DAPI | 4’,6-diamidino-2-phenylindole |
| dCK | Deoxycytidine kinase |
| dCTP | Deoxycytidine triphosphate |
| dFdC | 2’,2’-difluoro deoxycytidine |
| dFdCDP | Gemcitabine diphosphate |
| dFdCMP | Gemcitabine monophosphate |
| dFdCTP | Gemcitabine triphosphate |
| dFdU | 2’,2’-difluoro deoxyuridine |
| DHFU | Dihydro-fluorouracil |
| DMEM | Dulbecco’s modified Eagle’s medium |
| DMSO | Dimethyl sulfoxide |
| DNA | Deoxyribonucleic acid |
| DPD | Dihydropyrimidine dehydrogenase |
| dsRNA | Double-stranded ribonucleic acid |
| dUMP | Deoxyuridine monophosphate |
| ECM | Extracellular matrix |
| EDTA | Ethylene diamine tetraacetic acid |
| ELISA | Enzyme-linked immunosorbent assay |
| ETC | Electron transport chain |
| $FADH_2$ | Dihydroflavine-adenine dinucleotide |
| FBS | Fetal bovine serum |
| FdUMP | Fluorodeoxyuridine monophosphate |
| FdUTP | Fluorodeoxyuridine triphosphate |
| FOLFIRINOX | Folinic acid fluorouracil irinotecan oxaliplatin |
| FOXM1 | Forkhead box protein M1 |
| FUTP | Fluorouridine triphosphate |
| GAPDH | Gluceraldehyde-3-phosphate dehydrogenase |
| GEM-NAB | Gemcitabine combined with nanoparticle albumin-bound paclitaxel |
| GLUT1 | Glucose transporter 1 |
| HA | Hyaluronic acid |
| HBP | Hexosamine biosynthesis pathway |
| HCl | Hydrogen chloride |
| hCNT | Human concentrative nucleoside transporter |
| hENT | Human equilibrative nucleoside transporter |
| HEPES | 4-(2-hydroxyethyl)-1-piperaxineethanesulfonic acid |

| | |
|---|---|
| HIF | Hypoxia-induced factor |
| HP1 | Heterochromatin protein 1 |
| HRP | Horseradish peroxidase |
| hTERT | Human telomerase reverse transcriptase |
| iCAF | Inflammatory cancer-associated fibroblast |
| IL | Interleukin |
| IFP | Interstitial fluid pressure |
| IPMN | Intraductal papillary mucinous neoplasms |
| JAK | Janus kinase |
| KCl | Potassium chloride |
| KLF4 | Krüppel-like factor 4 |
| KRAS | Kirsten rat sarcoma viral oncogene homolog |
| KRH | Krebs-Singer-Hepes buffer |
| LDH | Lactate dehydrogenase |
| LDHA | Lactate dehydrogenase A |
| LG | Low glucose |
| MCT1 | Monocarboxylate transporter 1 |
| MCT4 | Monocarboxylate transporter 4 |
| $MgSO_4$ | Magnesium sulfate |
| MHCII | Major histocompatibility complex class II |
| MKRN1 | Makorin ring finger protein 1 |
| MLH1 | MutL homolog 1 |
| MMP | Metalloproteinase |
| MRI | Magnetic resonance imaging |
| mRNA | Messenger ribonucleic acid |
| miRNA | Micro ribonucleic acid |
| MSH2/6 | MutS homolog 2/6 |
| MTT | Thiazolyl blue tetrazolium bromide |
| myCAF | Myofibroblastic cancer-associated fibroblast |
| $N_2$ | Nitrogen |
| NaCl | Sodium chloride |
| NAD | Nicotinamide adenine dinucleotide |
| NADPH | Reduced nicotinamide adenine dinucleotide phosphate |
| NaOH | Sodium hydroxide |
| NF-κB | Nuclear factor-κB |
| NG | Normal glucose |

| | |
|---|---|
| NDPK | Nucleoside diphosphate kinase |
| NMPK | Nucleoside monophosphate kinase |
| NT | Nucleoside transporters |
| NTC | Non-targeting control |
| OXPHOS | Oxidative phosphorylation |
| PALB2 | Partner and localizer of breast cancer gene 2 |
| PanIN | Pancreatic intraepithelial neoplasia |
| PBS | Phosphate-buffered saline |
| PCC | Pancreatic cancer cell |
| PDAC | Pancreatic ductal adenocarcinoma |
| PDGF | Platelet-derived growth factor |
| PEP | Phosphoenolpyruvate |
| PGK1 | Phosphoglycerate kinase 1 |
| PGM | Phosphoglycerate mutase |
| PI3K | Phosphoinositide 3-kinase |
| PoI | Protein of interest |
| PON2 | Paraoxonase 2 |
| PP | Pancreatic polypeptide |
| PPP | Pentose phosphate pathway |
| PS | Penicillin-Streptomycin |
| PSC | Pancreatic stellate cell |
| PRSS1 | Serine protease 1 |
| PTEN | Phosphatase and tensin homolog |
| RB | Retinoblastoma |
| RNA | Ribonucleic acid |
| RNAi | Ribonucleic acid interference |
| RISC | Ribonucleic acid-induced silencing complex |
| ROS | Reactive oxygen species |
| RPM | Revolutions per minute |
| RRM1 | Ribonucleotide reductase |
| SDS-PAGE | Sodium dodecyl sulfate polyacrylamide gel electrophoresis |
| SEM | Standard error of the mean |
| SFM | Serum-free medium |
| SIR | Silent information regulator |
| siRNA | Small interfering ribonucleic acid |
| SLC | Solute carrier family |

| | |
|---|---|
| SLC2A1 | Solute carrier family 2 member 1 |
| SLC16A3 | Solute carrier family 16 member 3 |
| SMAD4 | Mothers against decapentaplegic homolog 4 |
| STAT | Signal transducer and activator of transcription |
| STK11 | Serine/threonine kinase 11 |
| SWI | Switch/sucrose non-fermentable |
| TBST | Tris-buffered saline containing 0.1% Tween 20 |
| TCA | Tricarboxylic acid cycle |
| TCR | T-cell receptor |
| TGF-β | Transforming growth factor-β |
| TMB | 3,3',5,5'-tetramethylbenzidine |
| TME | Tumor microenvironment |
| TP53 | Tumor protein 53 |
| TS | Thymidylate synthase |
| uTMP | Deoxythymidine monophosphate |
| ZEB1 | Zinc finger E-box homeobox 1 |
| ZEB2 | Zinc finger E-box homeobox 2 |
| αSMA | α-Smooth muscle actin |